Food Research International 209 (2025) 116196

Contents lists available at ScienceDirect

Food Research International

journal homepage: www.elsevier.com/locate/foodres

Hypoglycemic effect of dietary fibers from *Moringa oleifera* leaves: *In vitro* and *in vivo* studies

Xiufen Li [a,c,d,1], Jinye Yong [a,c,d,1], Bing Zhao [a,c,d], Yubo Zhu [a,c,d], Jia Luo [b,*], Jun Sheng [c,*], Yang Tian [a,c,d,e,*]

[a] College of Food Science and Technology, Yunnan Agricultural University, 425 Fengyuan Road, Kunming 650201, Yunnan, PR China
[b] Kunming Branch, CAS Key Laboratory of Tropical Plant Resource and Sustainable Use, Xishuangbanna Tropical Botanical Garden, Chinese Academy of Sciences, 88 Xuefu Road, Kunming 650223, Yunnan, PR China
[c] Engineering Research Center of Development and Utilization of Food and Drug Homologous Resources, Ministry of Education, Yunnan Agricultural University, 425 Fengyuan Road, Kunming 650201, Yunnan, PR China
[d] Yunnan Key Laboratory of Precision Nutrition and Personalized Food Manufacturing, Yunnan Agricultural University, 425 Fengyuan Road, Kunming 650201, Yunnan, PR China
[e] Pu'er University, Pu'er 665000, Yunnan, PR China

ARTICLE INFO

Keywords:
Moringa oleifera leaves
Dietary fiber
Hypoglycemia
Intestinal flora

ABSTRACT

Moringa leaf is traditionally regarded as a natural antagonistic diabetic herb in many countries. This study aimed to investigate the potential hypoglycemic activity of *Moringa* dietary fibers (MDFs) with different particle sizes *in vitro* and *in vivo* and reveal the related mechanisms. Among MDFs, MDF200 exhibited the highest glucose adsorption and diffusion retarding capacities and the most effective inhibition of digestive enzyme activities *in vitro*. All MDF interventions ameliorated insulin resistance and tissue damage, alleviated oxidative stress and dyslipidemia in high-fat diet and streptozotocin induced type 2 diabetes mice *in vivo*. MDF interventions, especially MDF80 and MDF200, remarkably promoted the diversity of cecum flora and the abundance of beneficial intestinal bacteria (*Ileibacterium, Bifidobacterium*), while inhibited the harmful bacteria (*Clostridium_sensu_stricto_1*). The ratio of *Firmicutes/Bacteroidetes* was significantly reduced by MDF40 and MDF80 interventions. MDF80 promoted fecal acetic acid, butyric acid and total short-chain fatty acids (SCFAs), while MDF40 promoted fecal propionic acid. All MDF interventions remarkably promoted the secretion of glucagon-like peptide-1 (GLP-1) and stimulated higher G protein-coupled receptor 43 (GPR43) protein expression in liver. Larger MDF activated phosphorylation of AMPK and Erk, while smaller MDF stimulated GLP-1, more PI3K and phosphorylation of Akt protein expression. These results revealed that MDFs ameliorated T2DM through modulating microbiota-SCFAs receptor (GPR43)/AMPK signaling pathways and stimulating GLP-1 secretion and activated liver PI3K/Akt signaling pathways. This study offers an effective case for MDFs as a potential dietary intervention or adjuvant treatment for type 2 diabetes and the application of *Moringa* leaf as a functional food material.

1. Introduction

As the data released by the diabetes atlas of the International Diabetes Federation in 2019, about 463 million adults contracted with diabetes in the world, which is expected to reach 578.4 million by 2030 and 700.2 million by 2045 (Thomas et al., 2019). China has the largest number of diabetic patients (estimated 113.9 million adults) in the world, which accounts for 24 % of the global patients (Li et al., 2020). Type 2 diabetes mellitus (T2DM), accounted for 90 % of all cases of diabetes, which characterized by high blood glucose, insulin resistance and beta cell failure (Ahmad, Lim, Lamptey, Webb, & Davies, 2022). The main causes of T2DM are unreasonable dietary habits, such as high sugar or fat but low dietary fiber diet (Zhao et al., 2018). Increased intake of dietary fibers is an attractive and practical strategy to prevent or alleviated T2DM without side-effects (Huang et al., 2022; Li et al., 2016; Li et al., 2018; Li et al., 2021; Li & Ma, 2024), compared with

* Corresponding author at: College of Food Science and Technology Yunnan Agricultural University, 425 Fengyuan Road, Kunming *650201*, Yunnan, PR China
E-mail addresses: luojia@xtbg.ac.cn (J. Luo), shengjun_ynau@163.com (J. Sheng), tianyang1208@163.com (Y. Tian).
[1] These authors contributed equally to this paper

https://doi.org/10.1016/j.foodres.2025.116196
Received 13 November 2024; Received in revised form 3 March 2025; Accepted 11 March 2025
Available online 22 March 2025

synthetic hypoglycemic drugs such as acarbose, insulin sensitizers, biguanides, sulfonylureas, *etc.*

The hypoglycemic effect of nature dietary fibers could be mainly attributed to selective promotion of the gut bacteria (Yu et al., 2023; Zhao et al., 2018), which influences the relative abundance and the diversity of their fermentation products, for instance, short-chain fatty acids (SCFAs), especially acetic acid, propionic acid and butyric acid (Zhao et al., 2018). These SCFAs act on SCFAs receptors (GPR40, GPR41 and GPR43) to regulate GPR43/AMPK and insulin signaling pathway (He et al., 2022). In addition, the hypoglycemic effect of nature dietary fibers is mainly attributed to the insoluble components and their fermentability (He et al., 2022; Li et al., 2016). Insoluble dietary fibers (IDFs) from enoki mushrooms, carrots and oats showed improved glucose tolerance and anti-hyperlipemia effect (Yang et al., 2021), which might be due to their high glucose adsorption capacity and glucose dialysis retardation index. Our previous study showed that insoluble dietary fiber from bamboo shoots exhibited the obesity prevention effect superior to several commonly consumed dietary fibers such as inulin, wheat fiber and soybean fiber (Li et al., 2016), which also promoted insulin sensitivity through Akt/AMPK/PGC-1α/p38 signaling in target tissues in high-fat diet mice, compared to equal amount of microcrystalline cellulose consumption (Li et al., 2018). Dietary fiber from tea residues exhibited effective hypoglycemic activities through modulating gut microbiota, enhancing SCFA level and improving the amino acid metabolism and citrate cycle (Huang et al., 2022). The anti-diabetic effects of carboxymethylated wheat bran dietary fiber in diabetic mice might be attributed to the improvement of insulin receptor activity and insulin signal transduction, promoting the synthesis of SCFAs to drive the regulation of gastrointestinal hormones and improving gut microbiota diversity (Li et al., 2021).

Moringa oleifera, has been used as food and useful herbal remedies for diabetes in Indian (Anwar et al., 2007; Vargas-Sánchez et al., 2019). It is a promising natural plant for the prevention and treatment of hyperglycemia and hyperlipidemia (Grosshagauer, Pirkwieser, Kraemer, & Somoza, 2021; Yang, Lin, & Zhao, 2023). In 2012, *M. oleifera* leaves was approved to be a new raw food material by Ministry of Public Health of China, due to its high nutritional feature and a variety of health-promoting effects (Yang, Tao, et al., 2023). The market of *Moringa* products was evaluated with 5.5 billion USD globally in 2017, in which *M. oleifera* leaf powder accounted for the largest market share (30 %) (Somoza et al., 2021). *M. oleifera* leaves are rich in dietary fiber (21–40 %, dry base), among which insoluble dietary fiber accounts for 19.6–34.9 % (dry base) and soluble dietary fiber content is 1.7–5.0 % (dry base) (Mallillin et al., 2014). Crude polysaccharides extracted from *M. oleifera* leaves using ultrasonic-assisted cellulase hydrolysis exhibited antioxidant and α-glucosidase inhibitory activities and alleviated the high glucose induced insulin resistance of HepG2 cells (Gu et al., 2022), while polysaccharides obtained using microwave-assisted extraction exhibited strong inhibitory activities on α-amylase and α-glucosidase (Chen et al., 2017). A high-purity polysaccharide extracted from *M. oleifera* Lam. leaf (Mw > 1000 kDa), which contains abundant arabinose and galactose, exhibited strong glycolipid absorption inhibitory activity and prebiotic effect on glycolipid metabolism related human gut probiotics (Yang, Lin, & Zhao, 2023). More obviously, a crude polysaccharide extracted from *M. oleifera* leaves, containing 38.90 % of total sugar and 48.70 % of total dietary fiber, showed obesity prevention activity in high-fat diet-fed mice through modulating gut microbiota (Li et al., 2022). However, the dietary fiber of *M. oleifera* is rarely studied as a single potential anti-diabetic substance. Whether the preventive and therapeutic functions of *M. oleifera* leaves on diabetes are due, or partly due, to its dietary fiber is still unclear.

Physicochemical and functional properties of polysaccharides or dietary fibers, such as solubility (Isken et al., 2010; Li et al., 2016; Luo et al., 2017), particle size (Jiang et al., 2022), water and oil holding capacity, glucose adsorption and dialysis retardation, inhibition on starch digestibility, α-amylase and α-glucosidase activities, showed a great influence on the hypoglycemic and hypolipidemic effects of dietary fibers (Jiang et al., 2022; Jin et al., 2019; Yang et al., 2021; Zhu et al., 2022). The reduced particle size of wheat bran insoluble dietary fiber resulted in altered fiber structure, improved hydration retention and gastrointestinal emptying capacity (Yang, Lin, & Zhao, 2023). As particle size decreased, the large surface area of insoluble dietary fiber increased the contact area between the fiber and glucose molecules, allowing glucose molecules to be retained on the fiber, thus inhibiting glucose diffusion (Zhang et al., 2024). More polar and non-polar groups (free hydroxyl groups, ether linkages and phenolic and carboxylic groups) exposed from the chains of smaller fiber resulted in more complicated interactions between dietary fiber and glucose molecules (Zhang et al., 2024). Besides, the effect of particle size of MDF on the regulation of gut microbiota and the related signaling pathways was still largely unknown. Therefore, the aim of this study was to investigate the hypoglycemic activity of *M. oleifera* dietary fibers (MDFs) with three particle sizes both in *in vitro* methods and in T2DM mice.

2. Materials and methods

2.1. Materials

The powdered *M. oleifera* leaf was supplied by Yunnan Tianyou Technology Co., Ltd. (Dehong, China). α-amylase, neutral protease, amyloglucosidase and α-glucosidase were purchased from Shanghai Yuanye Biotechnology Co., Ltd. Male C57BL/6 J mice were obtained from Beijing SiPeiFu Biotechnology Co., Ltd. Animal feed was purchased from Jiangsu Xietong Pharmaceutical Bio-engineering Co., Ltd. Streptozotocin and SCFA standards including acetic acid, propionic acid, butyric acid and isobutyric acid were purchased from Sigma-Aldrich Co. (Shanghai, China). Mouse insulin kit, BCA protein concentration detection kit, antibodies (AMPK, pAkt, Akt, GPR43, pErk, Erk) were purchased from Proteintech Biotechnology Co., Ltd. Antibodies (pAMPK and PI3K) were purchased from Cell Signaling Technology Co., Ltd.

2.2. Preparation, composition and microstructure analysis, and fourier transformed infrared spectroscopy (FTIR) of MDFs

M. oleifera leaf dietary fiber (MDF) was extracted according to the method of Nssor-Atindana et al. (Nsor-Atindana et al., 2012) with slightly modification. In brief, 50 g *M. oleifera* leaf powder was accurately weighed, mixed with 750 mL deionized water. The pH was adjusted to 6.0 by 0.6 mol/L HCI before adding α-amylase (3.75 g) in a water bath at 60 °C for 1 h. Then, the solution was adjusted to pH 7.0 with 1 mol/L NaOH before adding 1.5 g neutral protease. The mixture was incubated at 50 °C for 2.5 h. The pH was adjusted to 4.5, before adding 1.75 mL of glycosidase, and incubated at 40 °C for 1 h. Finally, the solution was boiled for 5 min to inactive the enzymes before cooling to room temperature. After centrifugation at 4000 *g* for 15 min, the precipitation was collected and washed with deionized water for 3 times, then freeze-dried to obtain the MDF. Moisture, protein, lipid, ash, total dietary fiber (TDF), soluble dietary fiber (SDF) and insoluble dietary fiber (IDF) contents were determined following the recommendations of the Official Methods of Analysis AOAC (Association of Official Analytical Chemists, 2005). Cellulose, hemicellulose and lignin contents were determined by Van Soest washing fiber method according to Emaga et al. (Emaga et al., 2008). The total phenol content was determined by the Folin-Ciocalteu method (Rumpf et al., 2023), and gallic acid was used as a standard. For microstructure analysis, the MDF was sprayed with gold for 45 s using a Quorum SC7620 sputter coater. Then, surface morphology of the sample was recorded under a scanning electron microscope (SEM, Regulus8100, Hitachi, Japan) with an accelerating voltage of 5.0 kV. The FTIR spectrum of MDF was recorded using an FTIR spectrophotometer (Nicolet IS10, Thermo Nicolet Ltd., USA). The MDF powder was sufficiently ground with KBr and pressed into a pellet. The FTIR spectrum of MDF was recorded following the

transmission pattern in the wavenumber range from 4000 to 400 cm^{-1} at a resolution level of 4 cm^{-1} and over 32 scans. Finally, the MDF was smashed and screened with 40-mesh sieve (630 μm, named MDF40), 80-mesh sieve (180 μm, named MDF80) and 200-mesh sieve (74 μm, named MDF200), respectively, for further analysis.

2.3. Evaluation of the functional properties of MDF: In vitro study

2.3.1. Water and oil holding capacity

Water holding capacity (WHC) and oil holding capacity (OHC) were measured according to the method of Lyu et al. (Lyu et al., 2021). One gram of MDF (W_1) was mixed with 20 mL deionized water or peanut oil in a dry centrifuge tube (W_0). For WHC, the tube was stored at room temperature for 24 h before centrifugation at 4000 *g* for 20 min. For OHC, the tube was stored for 18 h before centrifugation. The supernatant was removed, and the weight of the centrifuge tube was weighed again (W_2). The WHC or OHC was determined according to Eq. 1.

$$\text{WHC or OHC } (g/g) = \frac{(W_2 - W_0)}{W_1} \times 100 \quad (1)$$

2.3.2. Glucose adsorption capacity and glucose dialysis retardation index

Glucose adsorption capacity (GAC) and glucose dialysis retardation index (GDRI) of MDFs were determined using the method of Li et al. (Li, Liu, et al., 2022) with modifications. The details in GAC and GDRI measurement were described in the Supplementary material. The GAC and GDRI of each MDF were calculated as Eq. S1 and S2, respectively.

2.3.3. Starch digestibility inhibition activity

Alpha-amylase (10 mg) was added to 4 % potato starch solution (25 mL, dissolved in 0.05 mol/L phosphate buffer, pH 6.5) and mixed well with 0.25 g of MDF sample. The mixture was dialysed in 200 mL deionized water at 37 °C using the aforementioned dialysis bag. The glucose content in dialysate was measured within 240 min. Control group had no MDF in the dialysis bag (Ahmed et al., 2010). The effect of MDFs on starch digestion was expressed as the produced glucose.

2.3.4. The inhibition abilities of digestive enzymes

The inhibitory activities of MDF on α-amylase, α-glucosidase and pancreatic lipase were evaluated according to the methods of Benitez et al. (Benitez et al., 2019), Zheng et al. (Zheng et al., 2022) and Jiang et al. (Jiang et al., 2020), respectively. The inhibition rate of each digestive enzyme was calculated according to Eq. S3, S4 and S5, respectively. The detailed experimental protocol was supplied in the Supplementary material.

2.4. Animals and experimental design

Seventy 5-week-old C57BL/6 J mice (male, specific pathogen free) were purchased from Beijing SiPeiFu Biotechnology Co., Ltd. All mice were maintained in specific pathogen barrier facilities with controlled temperature (25 ± 2 °C) and light (12 h light-dark cycle). The relative humidity is 40–60 %. Standard food and distilled water were provided *ad libitum* throughout the experiment. Animal care and experimental processes were approved by the Institutional Animal Care and Use Committee of Yunnan Agricultural University with the permit number of 202307001.

After one week acclimatization, mice were randomly separated into 2 groups according to body weight. Control group (CON, $n = 10$) was given a normal diet (10 % energy from fat). Treatment groups were given a high-fat diet (60 % energy from fat, $n = 60$). After 4-week-feeding, mice were intraperitoneally injected with 50 mg/kg streptozotocin solution (STZ, dissolved in 0.1 mol/L, pH 4.5 cold citrate buffer, and injected within 30 min) for 3 consecutive days. The control group was intraperitoneally injected with 50 mg/kg cold citrate buffer (pH 4.5, injected within 30 min). Fasting blood glucose (FBG) was measured 3 and 10 days, respectively, after the last injection of STZ. Mice with FBG above 11.1 were considered as T2DM mice (Li et al., 2021), which were randomly divided into four groups (n = 10 each): high-fat diet group (HFD, diabetic model group), the metformin group (MET, positive control group), MDF40, MDF80 and MDF200 (*M. oleifera* leaf dietary fiber treatment groups), respectively. The MET group was orally administrated with 100 mg/kg metformin daily. HFD and three MDF treated groups orally administrated with equal amount sterile saline. In accordance with Zheng et al. (2022), 5 % dietary fiber amount was designed in the mouse experiment based on the basal standard research diet formulation (D12492). HFD and MET groups were fed high-fat diet containing 5 % microcrystalline cellulose, while three MDF groups fed high-fat diet containing 5 % MDF40, MDF80, and MDF200, respectively. The experimental diets were listed in Table S1. Food intake, body weight, and FBG were recorded weekly.

2.5. Tissue collection and biochemical analysis

After 5 weeks of MDF intervention, the mice were fasted overnight and weighed before execution. Blood samples were collected and centrifuged at 3000 *g* for 10 min (4 °C). The supernatant was obtained and stored at −80 °C for biochemical analysis. Mouse liver, pancreas, adipose tissue, spleen and kidney were weighted. A small part of liver, colon and pancreas were fixed in 4 % paraformaldehyde solution for 48 h before embedded in paraffin wax for preparing tissue slice (2–3 μm). Then, the slice was stained with hematoxylin & eosin (H&E) for histopathological analysis. Eight mice from each group were randomly selected, and fresh feces from mouse cecum were collected, frozen in liquid nitrogen immediately for 16S rRNA sequencing. Feces in colon near the cecum were collected for the determination of SCFAs content. Total triglyceride (TG), total cholesterol (TC), high density lipoprotein cholesterol (—HDL-C), low density lipoprotein cholesterol (LDL-C) and malondialdehyde (MDA) concentrations in serum were determined using the commercial kit (Nanjing Jiancheng Institute of Bioengineering, Nanjing, China), respectively. The activities of superoxide dismutase (SOD), and glutathione peroxidase (GSH-P_X) in serum were determined using the corresponding detection kit (Nanjing Jiancheng Institute of Bioengineering). Serum insulin and glucagon like peptide-1 (GLP-1) levels were determined by enzyme-linked immunosorbent assay with different kits from Wuhan Sanying Biotechnology Co., LTD. And Wuhan Aibotek Biotechnology Co., LTD., respectively. The homeostasis model assessment of insulin resistance (HOMA-IR) index was calculated according to Eq. (8) (Xiang et al., 2021):

$$\text{HOMA} - \text{IR} = \frac{\text{FBG} \times \text{Insulin}}{22.5} \quad (8)$$

2.6. Glucose and insulin tolerance tests

Oral glucose tolerance test (GTT) and insulin tolerance test (ITT) were performed for 1 week before execution. For GTT test, the mice were fasting overnight before the determination. Blood glucose levels were measured before and after 30 min, 60 min, 90 min and 120 min of gavage with 10 % glucose solution, respectively. For ITT test, mice were fasted for 6 h. Blood glucose levels were measured before and after 30 min, 60 min, 90 min and 120 min of insulin (0.5 U/kg) injection, respectively. For both tests, the area under the curve (AUC) was calculated.

2.7. Western blot analysis

The liver tissues (0.02 g) were homogenized in cool RIPA lysis buffer (200 μL), The homogenate was centrifuged at 12,000 *g* for 5 min (4 °C). The supernatant was collected, and the protein concentration was determined by a BCA protein assay kit (Nanjing Jiancheng Bioengineering Institute, Nanjing, China). The protein (60 μg) was separated by

10 % SDS-PAGE and transferred to a polyvinylidene difluoride (PVDF) membrane, followed by blocking with 5 % skimmed milk in 0.5 % TBST (PBS with 0.1 % Tween 20) for 2 h at room temperature. Then, the PVDF was incubated with the primary antibodies (pAMPK, AMPK, pAkt, Akt, GPR43, PI3K pErk, Erk and β-actin, respectively) overnight at 4 °C. After washed with TBST, the membranes were incubated with horseradish peroxidase-conjugated secondary antibodies for 2 h. Finally, the protein bands were visualized by enhanced ECL reagents and quantified using Image Lab software for density detection.

2.8. 16S rRNA sequencing

Total bacterial genomic DNA was extracted from the feces using a QIAamp DNA Stool minikit (Qiagen, Hilden, Germany) following the manufacturer's instructions. The integrity of extracted genomic DNA was detected by 1 % agarose gel electrophoresis. The V4 region was amplified with the 16S rRNA gene forward primer 338F (5'-ACTCC-TACGGGAGGCAGCAG-3′) and reverse primer 806R (5'-GGAC-TACHVGGGTWTCTAAT) before 16S rRNA gene sequencing by using Illumina MiSeq PE300 platform (Illumina, San Diego, USA). The 16S rRNA data were analyzed on the online platform of Majorbio Cloud Platform (https://www.majorbio.com). Correlations between gut microbiota (significant changed at genus level) and other metabolic parameters were visualized with Spearman's correlation using a programming language R (V4.0.0, AT&T Bell Laboratories New Zealand).

2.9. Fecal SCFAs determination

The SCFAs in the feces were determined by Agilent —8890B-5977B GC/MSD according to the previously reported method (Hsu et al., 2019). Briefly, fecal samples (20 mg) were homogenized with 800 μL phosphoric acid (0.5 %, containing 2-ethylbutyric acid, 10 μg/mL) for 3 min (50 Hz), ultrasound for 10 min, and then centrifuged at 13,000 *g* for 15 min. The supernatant (200 μL) was collected and mixed with *n*-butanol (200 μL) for 10 s, ultrasound for 10 min at 4 °C, and centrifuged (13,000 *g*, 5 min at 4 °C). The supernatant was obtained and filtered for GC–MS analysis. The chromatographic conditions: HP FFAP capillary column (30 m × 0.25 mm × 0.25 μm, Agilent J&W Scientific, Folsom, CA, USA) with high purity helium as carrier gas, flow rate of 1 mL/min, inlet temperature of 180 °C, sample size of 1 μL. Acetic acid, propanoic acid, butanoic acid, isobutanoic acid, valeric acid, isovasleric acid, hexanoic acid, isohexanoic acid were used as standard samples.

2.10. Statistical analysis

All data were analyzed by SPSS Statistics 26.0 software (SPSS Inc., Chicago, IL, USA) and expressed as mean ± standard deviation. One-way ANOVA followed by Turkey's test was used to analyze the data. A *P*-value <0.05 was considered to be statistically difference.

3. Results

3.1. Main components and in vitro functional properties of MDFs

Main components, microstructure and the FTIR spectrum of MDF. The main components of MDF are shown in Table 1. The extraction rate of dietary fiber were 44.7 %. The TDF content of MDF is 75.46 %, including 68.95 % IDF and 6.50 % SDF. Other basic components of MDF include 11.56 % protein, 6.69 % ash, 3.95 % water and 0.84 % fat. In respect of chemical fiber content, cellulose (37.47 %) was the highest, followed by lignin (16.76 %) and hemicellulose (11.23 %) (Table 1). The microstructure of MDF was further observed by SEM as shown in Fig. S1. The surface structure of MDF was porous (Fig. S1A) with a loose and intertwined network structure (Fig. S1B). The porous structure of insoluble dietary fiber favors affinity adsorption to glucose molecules and glucose retention in the small intestine, thereby regulating blood glucose levels

Table 1
Main components of MDF.

Main component		Content (%)
Base component	Moisture	3.95 ± 0.31
	Protein	11.56 ± 1.66
	Ash	6.69 ± 0.04
	Fat	0.84 ± 0.00
	Total dietary fiber (TDF)	75.46 ± 2.58
Dietary fibers	Insoluble dietary fiber (IDF)	68.95 ± 1.84
	Soluble dietary fiber (SDF)	6.50 ± 3.99
	Cellulose	37.47 ± 5.59
Chemical fibers	Hemicellulose	11.23 ± 1.02
	Lignin	16.76 ± 1.97

Note: Different letters (a-b) indicate significant differences ($P < 0.05$).

(Zhang et al., 2024). From *FTIR* spectrum (Fig. S2), the broad absorption at around 3362 cm^{-1}, was attributed to the stretching vibration of hydroxyl group in native cellulose. The prominent absorption at 2918 cm^{-1} was due to the C—H stretching of -CH_3 or = CH_2, which represented the typical structure of cellulosic polysaccharides (Hua et al., 2019). The minor peak at 1741 cm^{-1} was mainly due to the characteristic C═O stretching vibration of hemicellulose. The prominent peak at 1633 cm^{-1} was representative of the esterified and ionized carboxyl groups of uronic acid (Jiang et al., 2020). The weak peak at 1551 cm^{-1}, together with the minor peak at 1434 cm^{-1}, was a result of the aliphatic or aromatic C—H group vibration of lignin. The sharp peak at 1318 cm^{-1} was mainly from the typical cellulose structure. The weak peak at 1244 cm^{-1} was correspond to the O—H or C—O group vibration of cellulose or hemicellulose. The absorption at 1066 cm^{-1} originated from the acyloxygen (CO–OR) stretching vibration of hemicelluloses and the C—O stretching vibration of lignin (Hua et al., 2019). Thus, the *FTIR* spectrum of MDF showed typical insoluble cellulose and hemicellulose and lignin, which was confirmed by the results in Table 1.

WHC and OHC of MDFs. Physicochemical properties of dietary fibers are closely related to their beneficial effects in disease (Li & Ma, 2024). Water and oil retention are important indexes to evaluate the functional properties of dietary fibers. As shown in Fig. 1A, three MDFs showed WHC values of 4.62 g/g, 4.66 g/g and 4.86 g/g, respectively, exhibiting higher water retention of MDFs. Moreover, the WHC of MDF200 was significantly higher than MDF40 and MDF80 ($P < 0.05$). Oil binding capacity (OBC) assesses the ability of dietary fiber to prevent the loss of oil during food processing and the ability to reduce serum cholesterol by binding fat or oil in human digestive system (Hua et al., 2019). As shown in Fig. 1B, the OHC of MDFs was 3.34–3.39 g/g without significant difference among different MDFs.

Glucose adsorption capacity (GAC), glucose dialysis retardation index (GDRI), and effect of MDFs on starch digestibility. As shown in Fig. 1C, the adsorption amount of MDF increased with the increasing of glucose concentration (5–100 mmol/L). In lower glucose concentrations (5 mmol/L and 10 mmol/L), the GAC of MDF showed no significant difference, while a particle size-dependent adsorption manner was observed in higher glucose concentrations (50 mmol/L and 100 mmol/L) (Fig. 1C). GDRI is a useful index for predicting the effect of dietary fiber on glucose diffusion (Benitez et al., 2019; Nsor-Atindana et al., 2012). Fig. 1D showed the time-dependent impact of MDF on glucose diffusion. All MDFs exhibited clear inhibitory effects on glucose diffusion, compared to the control (without dietary fiber), with the GDRI order of MDF200 > MDF80 > MDF40 (Fig. 1D). MDF80 and MDF200 showed the higher GDRI during dialysis time from 30 min to 150 min than MDF40, which indicated that smaller MDF particle was more effective in inhibition of glucose diffusion. The better inhibitory effect of small fiber particles was probably due to the increased physical barrier and more trapped glucose with smaller MDF to prevent glucose diffusion (Benitez et al., 2019). Fig. 1E showed that MDFs lowered the glucose in the dialysate after 1 h (MDF200 ≤ MDF80 ≤ MDF40), while this trend was not obvious during 2–4 h dialysis, except for MDF200 (Fig. 1E),

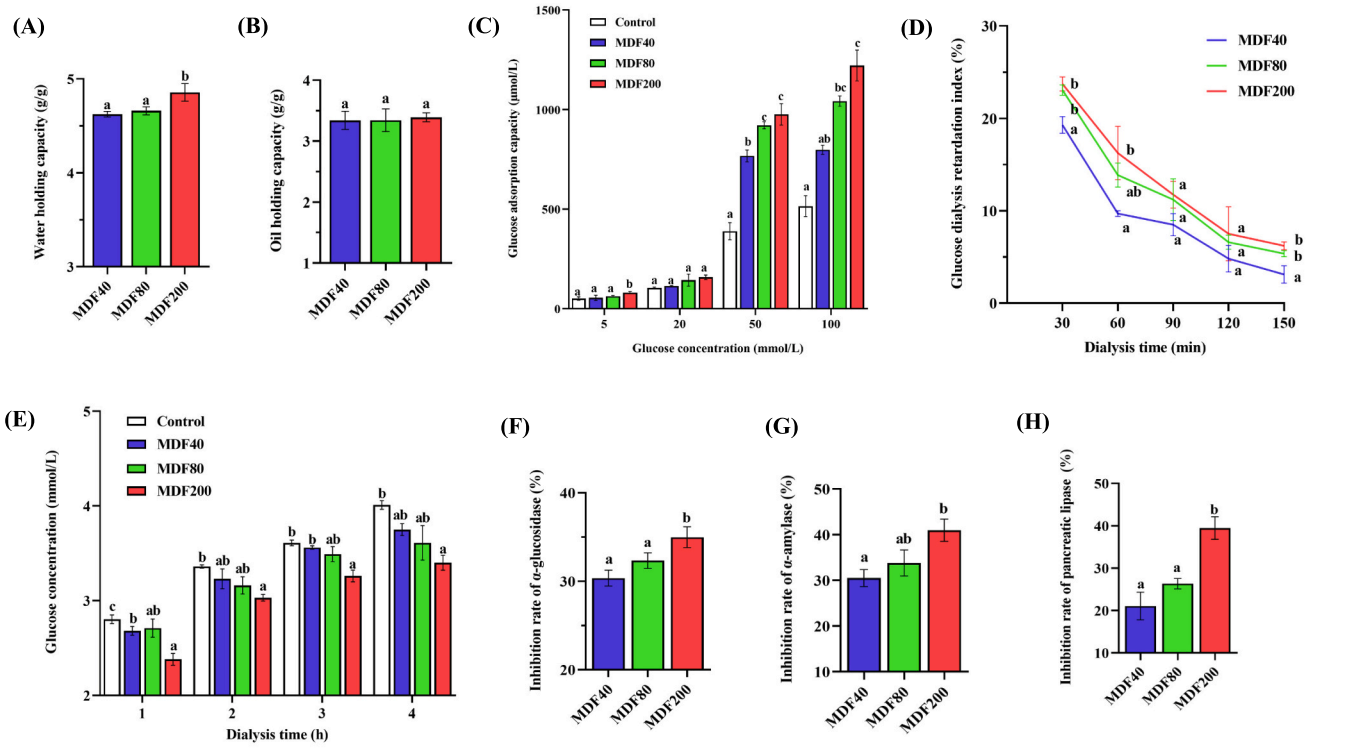

Fig. 1. Functional properties of MDF. Water (A) and oil (B) holding capacities of MDFs. Glucose adsorption capacity (C) and the retardation effect of MDFs on glucose dialysis (D). Inhibitory effect of MDFs on starch digestibility (E). Inhibition effects of MDFs on α-amylase (F), α-glucosidase (G) and pancreatic lipase (H). Data were presented as mean ± SD ($n = 3$). Different letters indicate significant differences ($P < 0.05$).

compared with the control group. Results indicated that MDFs effectively inhibited starch digestion, especially MDF200.

Effect of MDFs on α-glucosidase, α-amylase and pancreatic lipase activities. Alpha-glucosidase is an important endogenous hydrolase in human body, which plays a crucial role in the process of converting carbohydrates to glucose. From Fig. 1F, all MDFs inhibited the activity of α-glucosidase, with inhibition rates of 30.36 %, 32.34 % and 34.98 % for MDF40, MDF80 and MDF200, respectively. This indicated that the decrease of particle size of MDF increased the inhibition rate for α-glucosidase. MDF200 showed the most effective inhibition on the activity of α-glucosidase, which was significantly higher than those of MDF80 and MDF40 ($P < 0.05$). Inhibition of α-amylase activity would prolong the digestion time of starch and reduce the rate of glucose production in the small intestine, thus be beneficial for the effective control of postprandial blood glucose. From Fig. 1G, all MDFs inhibited the activity of α-amylase, with a trend negatively related to the particle size. Pancreatic lipase plays a key role in the digestion of triglycerides. The inhibition of pancreatic lipase prevents the absorption of triglycerides in intestine, which is a way to control hyperlipidemia and obesity (Xue et al., 2020). As shown in Fig. 1H, the inhibition rate of MDFs on pancreatic lipase was at high level, with 22.03 %, 26.41 % and 39.46 % for MDF40, MDF80, and MDF200, respectively. The inhibition rate of MDF200 was the highest among the tested MDFs ($P < 0.05$).

3.2. Food and water intake, organ morphology, serum lipids and oxidative stress

Food and water intake. After 5 weeks of MDF diet intervention, the body weight of mice in all high-fat groups was significantly reduced ($P < 0.05$, Fig. S3A) compared with that of control group. Food intake of mice was decreased in both MET, MDF40 and MDF80 groups, compared with HFD (Fig. S3B), while water intakes of mice in all high-fat groups were all increased (Fig. S3C).

Organ morphology. Liver and pancreas weight in HFD group were significantly increased ($P < 0.05$, Table 2), compared with those of control group. Under microscope, large numbers of hepatocyte steatosis and fat vacuoles were observed in HFD group, compared to the uniform and order arrangement in control group (Fig. 2A). The islet in pancreas of HFD group was atrophied with blurred, irregular and severely reduced size, compared to the big and round islet in control group. After 5 weeks of MDF diet intervention, all MDFs treated groups showed a decreasing trend in liver weight (Table 2) and less fat vacuole among hepatocyte, indicating that changes in liver were slightly reversed. In these groups, the volume of mouse islets restored largely, which were comparable to the MET group. In addition, diabetes also affects the structure and function of colon, which can lead to gastrointestinal symptoms such as constipation, diarrhea, bloating, and abdominal pain. Compared with control group, colonic epithelial cells of mice in HFD group were damaged, goblet cells were reduced, and crypt structure was changed, suggesting the intestinal damage and possible barrier dysfunction. In MDFs treated groups, the morphology of epithelial and goblet cells was significantly restored, indicating an amelioration effect of MDFs on colon tissue.

Serum lipids and oxidative stress. Compared with the control group, TG, TC and LDL-C were significantly increased in HFD group ($P < 0.05$, Fig. 2B, C and D), while these serum lipid parameters were significantly reduced in all MDFs treated groups. Moreover, HDL-C is a protective factor against atherosclerosis and coronary heart disease (Thomas et al., 2019). HDL-C level was significantly increased in all MDFs treated and MET groups ($P < 0.05$, Fig. 2E), although no difference was observed in HFD group compared to control group. The result indicated that MDFs all had beneficial effect in improving lipid profiles. Another serious consequence of persistent high blood sugar caused by T2DM is severe oxidative stress and tissue damage in the body (Huang et al., 2022). Thus, SOD and GSH-P_X are considered to be the first line of defense against free radicals generated in body (Jin et al., 2019). Compared with

Table 2
Effects of MDF on organ index in mice.

Group	Liver (%)	Pancreatic (%)	Cardiac (%)	Spleen (%)	Renal (%)	Perirenal fat (%)	Epididymal fat (%)
CON	3.47 ± 0.20^{a}	0.67 ± 0.09^{a}	0.52 ± 0.04^{a}	0.62 ± 0.19^{b}	1.19 ± 0.06^{b}	0.32 ± 0.10^{a}	1.34 ± 0.68^{a}
HFD	4.02 ± 0.30^{b}	0.95 ± 0.18^{b}	0.51 ± 0.05^{a}	0.61 ± 0.12^{b}	1.02 ± 0.05^{a}	0.39 ± 0.15^{a}	1.29 ± 0.34^{a}
MET	4.08 ± 0.27^{b}	0.77 ± 0.19^{ab}	0.54 ± 0.08^{a}	0.60 ± 0.11^{b}	1.07 ± 0.06^{a}	0.36 ± 0.14^{a}	1.23 ± 0.38^{a}
MDF40	3.72 ± 0.30^{ab}	0.84 ± 0.28^{ab}	0.49 ± 0.03^{a}	0.52 ± 0.15^{ab}	1.05 ± 0.05^{a}	0.35 ± 0.18^{a}	1.24 ± 0.43^{a}
MDF80	3.84 ± 0.25^{ab}	1.00 ± 0.18^{b}	0.53 ± 0.05^{a}	0.59 ± 0.10^{b}	1.07 ± 0.07^{a}	0.32 ± 0.12^{a}	1.10 ± 0.22^{a}
MDF200	3.74 ± 0.41^{ab}	0.90 ± 0.20^{ab}	0.53 ± 0.08^{a}	0.41 ± 0.06^{a}	1.04 ± 0.09^{a}	0.31 ± 0.10^{a}	1.10 ± 0.31^{a}

Note: Different letters (a-b) indicate significant differences ($P < 0.05$).

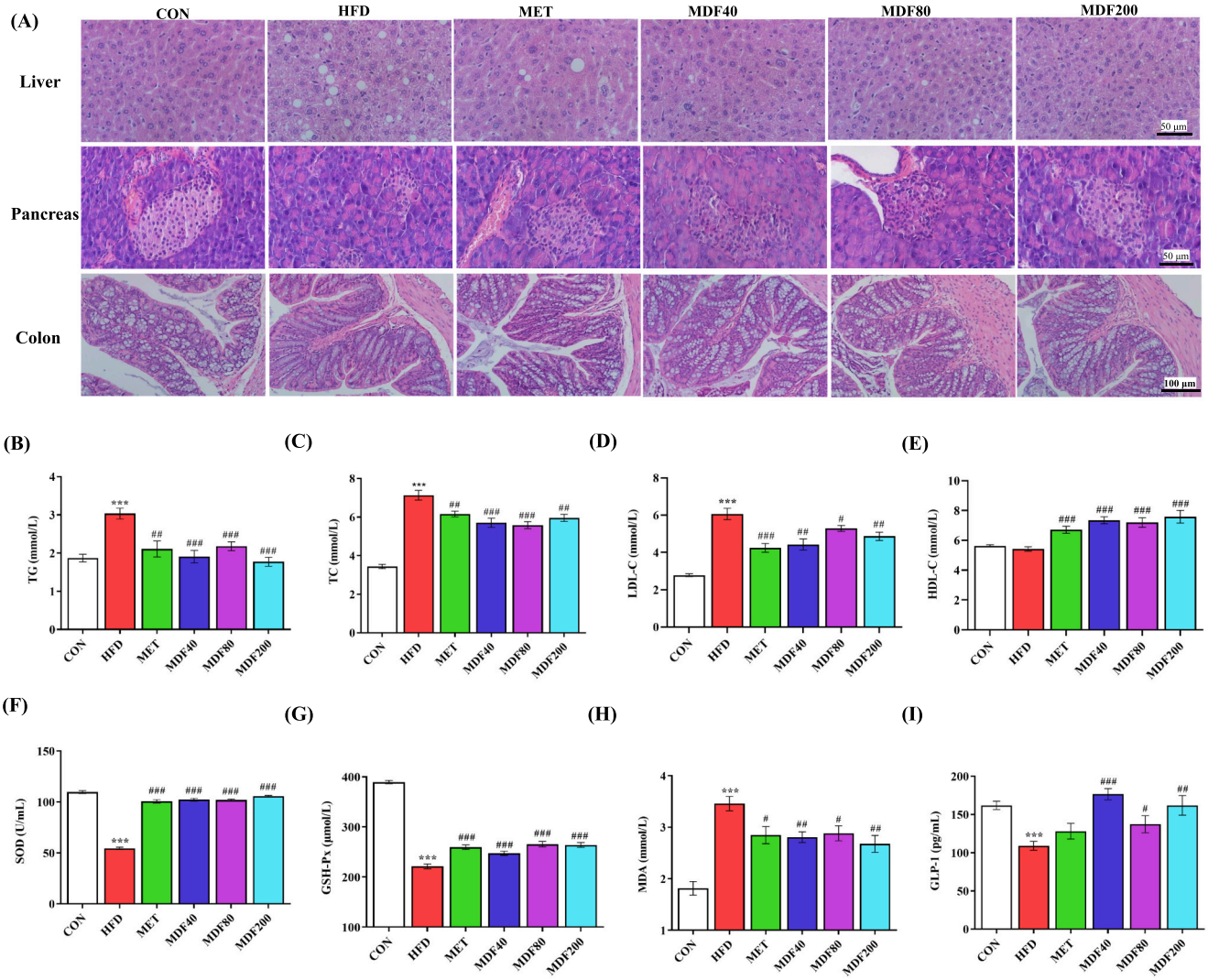

Fig. 2. Effect of MDFs on organ morphology and biochemical parameters in T2DM C57BL/6 mice. (A) H&E staining of mouse liver, pancreas and colon. (B) Triglyceride (TG), (C) Total cholesterol (TC), (D) HDL cholesterol (HDL—C) and (E) LDL cholesterol (LDL-C) levels in mice serum. (F) SOD, (G) GSH-Px, (H) MDA and (I) Serum glucagon like peptide-1 (GLP-1). Data were presented as mean ± SEM ($n = 8$). CON, control group; HFD, diabetic model group; MET, positive control group, MDF40, MDF80 and MDF200, *M. oleifera* leaf dietary fiber treatment groups. $^{***}P < 0.001$ compared with CON, and $^{\#}P < 0.05$, $^{\#\#}P < 0.01$, $^{\#\#\#}P < 0.001$ compared with HFD.

control group, serum SOD and GSH-P_X levels of mice in HFD group were significantly decreased, while serum MDA level was largely increased ($P < 0.05$, Fig. 2F and G). After 5-week MDF intervention, the activities of SOD and GSH-P_X in serum of MDF groups were significantly increased, while the content of MDA was significantly decreased ($P < 0.05$, Fig. 2H). These results indicated that dietary MDFs protected mice from hyperglycemia induced oxidative stress.

GLP-1, an insulin-like hormone that stimulates pancreatic beta cells to secrete insulin in a glucose-dependent manner, plays an important role in weight control, glucose homeostasis and nutrient metabolism (Wang et al., 2021). Hence, increasing and stabilizing GLP-1 levels is an important strategy for T2DM control. Compared with control group, serum GLP-1 level in HFD group was significantly decreased ($P < 0.05$, Fig. 2I). This level was effectively increased after MDF interventions ($P < 0.05$, Fig. 2I). Combined the results from Fig. 2, it can be inferred that the increase of GLP-1 level in mice by MDFs may have a certain promoting effect on regulating body weight, promoting proliferation or regeneration of β cells, increasing insulin level and improving glucose

homeostasis and lipid metabolism in mice.

3.3. Glucose, insulin and glucose tolerance test

After 5-week intervention, FBG level in HFD group was significantly higher than that in control group ($P < 0.001$, Fig. 3A). Compared with HFD group, the FBG of MDF groups was significantly reduced ($P < 0.01$, Fig. 3A), similar to that of metformin group. Insulin is an important hypoglycemic hormone in maintaining glucose homeostasis. Compared with control group, fasting insulin of mice in HFD group significantly decreased, while fasting insulin of mice was restored significantly in MDF groups ($P < 0.001$, Fig. 3B). Insulin resistance is a prominent feature of diabetes. In the compensation stage of diabetes, different degrees of insulin resistance often appear in animal models of T2DM mice (Tu et al., 2019). As shown in Fig. 3C, HOMA-IR index of HFD group was significantly higher than that of control group ($P < 0.001$), indicating insulin resistance in HFD mice. After dietary intervention of MDF40 and MDF200, HOMA-IR index was significantly lowered ($P < 0.05$, Fig. 3C) indicating improvement of insulin resistance, similar to the effect of metformin.

Oral glucose tolerance test (GTT) is used to assess islet beta cell function and glucose regulation. From the GTT curve (Fig. 3D), blood glucose of all groups reached the maximum after 30 min before glucose intragastric administration. The blood glucose level of mice in HFD group was significantly higher than that in control group (Fig. 3D), which was verified by the area under the curve (AUC, $P < 0.001$, Fig. 3E), indicating that the glucose tolerance of mice in HFD group was seriously impaired. Compared with HFD group, AUC values in MDF treated groups were significantly decreased ($P < 0.001$), indicating the improvement of glucose sensibility in mice. Fig. 3F depicted the results of insulin tolerance test (ITT). After insulin injection, the blood glucose of all groups was reduced. The AUC value of mice in HFD group was significantly higher than that in control group ($P < 0.001$, Fig. 3G), indicating that insulin resistance of mice in HFD group was serious. Compared with HFD group, the AUC value of mice in MDF40 group was significantly decreased ($P < 0.05$), which was comparable to the value in MET group. This result indicated that MDF40 alleviated insulin resistance in T2DM mice.

3.4. Protein expressions of pAMPK/AMPK, GPR43, pAkt/Akt and pErk/Erk

To further investigate the potential hypoglycemic mechanism of MDFs, protein expressions in insulin signaling pathways were determined, as shown in Fig. 4. In HFD group, liver GPR43 and pAMPK/AMPK protein levels were lower than those in control group ($P < 0.05$, Fig. 4A). Compared to HFD group, MDF40 and MDF80 interventions increased the expression of pAMPK by 119 % ($P < 0.05$) and 55 % ($P < 0.01$), respectively. Compared to HFD group, MDF40, MDF80 and MDF200 interventions significantly increased the protein expression of GPR43 by 113 % ($P < 0.05$), 146 % ($P < 0.01$), and 200 % ($P < 0.001$, Fig. 4A), respectively.

In insulin signaling pathway, Akt mediates glucose transport, glycogen and protein synthesis, lipogeneisis in liver tissue (He et al., 2022). In HFD group, liver protein expressions of pAkt and PI3K were significantly lower than those in control group ($P < 0.05$, Fig. 4B). Compared to HFD group, the level of pAkt was enhanced in MDF200 ($P < 0.05$), while the level of PI3K was elevated in MDF80 and MDF200 groups ($P < 0.05$). These results indicated that MDF intervention increased the phosphorylation levels of AMPK and AKT and the protein

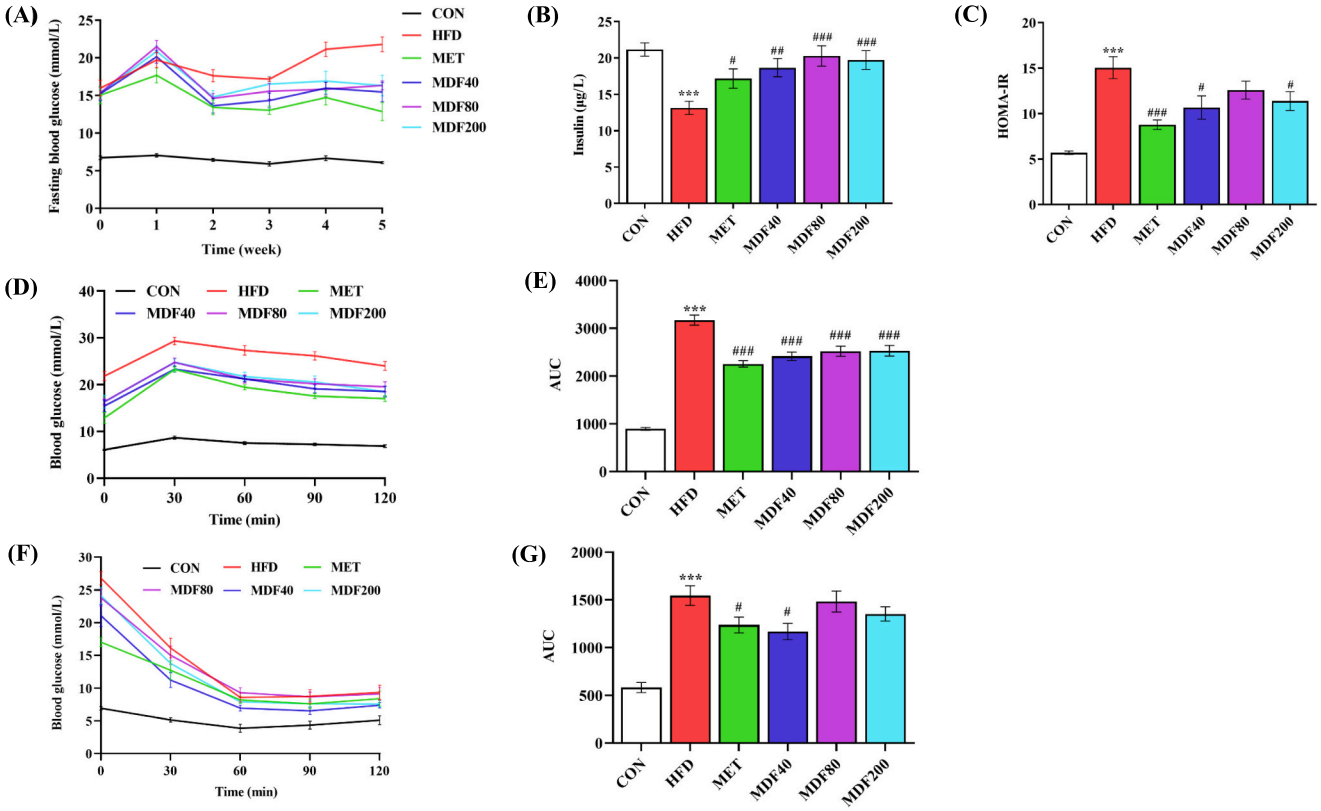

Fig. 3. Effect of MDFs on glucose homeostasis in T2DM C57BL/6 mice. Fasting blood glucose during 5-week treatment (A). Serum insulin (B) and homeostasis index of insulin resistance (HOMA-IR) (C). Glucose tolerance test (D) and the area under the curve (AUC) (E). Insulin tolerance test (F) and the area under the curve (AUC) (G). Data were presented as mean ± SEM (n = 8). CON, control group. HFD, diabetic model group. MET, positive control group. MDF40, MDF80 and MDF200, *M. oleifera* leaf dietary fiber treatment groups. $^{***}P < 0.001$ compared with CON. $^{\#}P < 0.05$ compared with HFD.

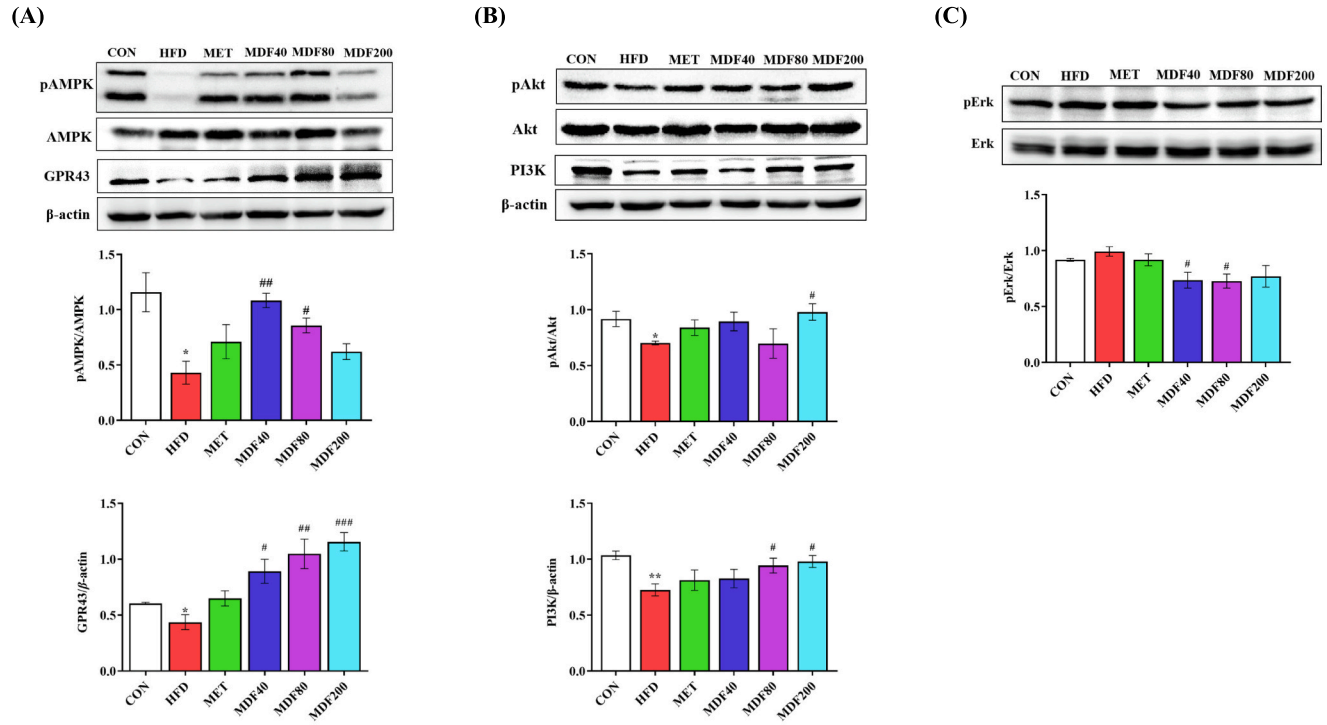

Fig. 4. Effect of MDFs on GPR43-AMP-activated protein kinase (AMPK), Akt-PI3K and Erk signalings in liver. (A) The protein expressions of pAMPK/AMPK and GPR43/β-actin. (B) The protein expressions of pAkt/Akt and PI3K/β-actin. (C) The protein expression of pErk/Erk. CON, control group; HFD, diabetic model group; MET, positive control group, MDF40, MDF80 and MDF200, *M. oleifera* leaf dietary fiber treatment groups. $^{*}P < 0.05$, $^{**}P < 0.01$ compared with CON, and $^{\#}P < 0.05$, $^{\#\#}P < 0.01$, $^{\#\#\#}P < 0.001$ compared with HFD.

expressions of GPR43 and PI3K in liver of mice. In addition, Erk phosphorylation is involved in the development of dyslipidemia induced by STZ in T2DM mice (Xu et al., 2018). An abnormal activation trend of Erk was observed in HFD group, which was reversed in MDF40 and MDF80 groups (pErk/Erk, $P < 0.05$, Fig. 4C), supporting the recovery of serum lipid levels after MDFs treatment (Fig. 2). The results indicated that MDFs improved lipid distribution by inhibiting Erk phosphorylation in the liver tissue in mice.

3.5. Fecal SCFAs concentration and microbiota diversity

SCFAs, mainly including acetic acid, propionic acid, butyric acid, *etc.*, are produced by gut microorganisms, involving in regulating insulin secretion and maintaining glucose homeostasis. Compared with mice in control group, fecal acetic acid and total SCFAs levels were significantly reduced in HFD group ($P < 0.05$, Fig. 5A and D). After MDFs treatment, fecal acetic acid, butyric acid and total SCFAs were significantly reversed in MDF80 group ($P < 0.05$, Fig. 5A, C and D) when compared with HFD group. Moreover, propionic acid was significantly restored in MDF40 mice ($P < 0.05$, Fig. 5B).

After 5-weeks MDF intervention, the principal coordinate analysis (PCoA) of microbial colony similarity was shown in Fig. 5E. The PC1 and PC2 accounted for 29.57 % and 15.31 % of the total variance, respectively. The PCoA diagram showed obvious separability and spatial aggregation. There were significant differences in microflora characterized by different treatment groups. The weighted UniFrac distance of the HFD group and the MET group overlapped, while the weighted UniFrac distance of three MDF groups and the control group were closer. These results indicated that MDF intervention improved the structure of intestinal flora in diabetic mice. Alpha-diversity index was calculated to know if differences in dietary fiber led to changes in gut microbial diversity. Compared with control group, only shannon index was significantly increased in HFD group, while no difference was observed for Ace, Chao and Simpson indexes (Fig. 5F-I). These results indicated that the diversity of microbiota in HFD was comparable to that of control group. However, after 5-week dietary intervention, Ace and Shannon indexes were significantly increased in both MDF80 and MDF200 groups (Fig. 5F and H). Chao index was significantly increased only in MDF80 group (Fig. 5G). Simpson index was significantly decreased in all MDFs ($P < 0.05$, Fig. 5I). The results indicated that MDFs improved the diversity of intestinal flora in T2DM mice.

3.6. Microbial abundance and its correlation with physiological indexes

At the phylum level, *Firmicutes*, *Actinobacteria*, *Desulfobacterota*, *Patescibacteria*, and *Bacteroidetes* rank among the top 5. Among them, *Firmicutes* accounted for the largest, followed by *Bacteroidetes* (Fig. S2). The ratio of *Firmicutes/Bacteroides* is considered to be an indicator of intestinal microbial dysbiosis, which is positively associated with insulin resistance and obesity (He et al., 2022; Li et al., 2016). Compared with control group, the relative abundance of *Firmicutes* was significantly increased in HFD group ($P < 0.05$), while fell back in all MDF groups (Fig. 6A). Adversely, the relative abundance of *Bacteroidetes* was significantly decreased in HFD group ($P < 0.01$), while significantly increased in MDF40 and MDF80 groups (Fig. 6B). The ratio of *Firmicutes/Bacteroidetes* was largely augmented in HFD group ($P < 0.01$, Fig. 6C), while reverted in MDF80 and MDF200 ($P < 0.05$). These results suggest that MDFs may ameliorate intestinal flora imbalance in T2DM mice.

At the genus level, compared to the control, the relative abundance of *Faecalibaculum*, *Lactobacillus*, *Dubosiella*, *Romboutsia*, unclassified_f_*Lachnospiraceae* and *Clostridium_sensu_stricto*_1 were increased in the HFD group, while the relative abundance of *Ileibacterium*, *Bifidobacterium*, *Coriobacteriaceae*_UCG-002 and *Desulfovibrio* were significantly decreased (Fig. 6D and E). After the ingestion of MDF, the relative abundance of *Clostridium_sensu_stricto*_1, unclassified_f_*Lachnospiraceae* and *Faecalibaculum* decreased, while the abundance of beneficial bacteria *Ileibacterium* and *Romboutsia* were largely increased ($P < 0.05$) in

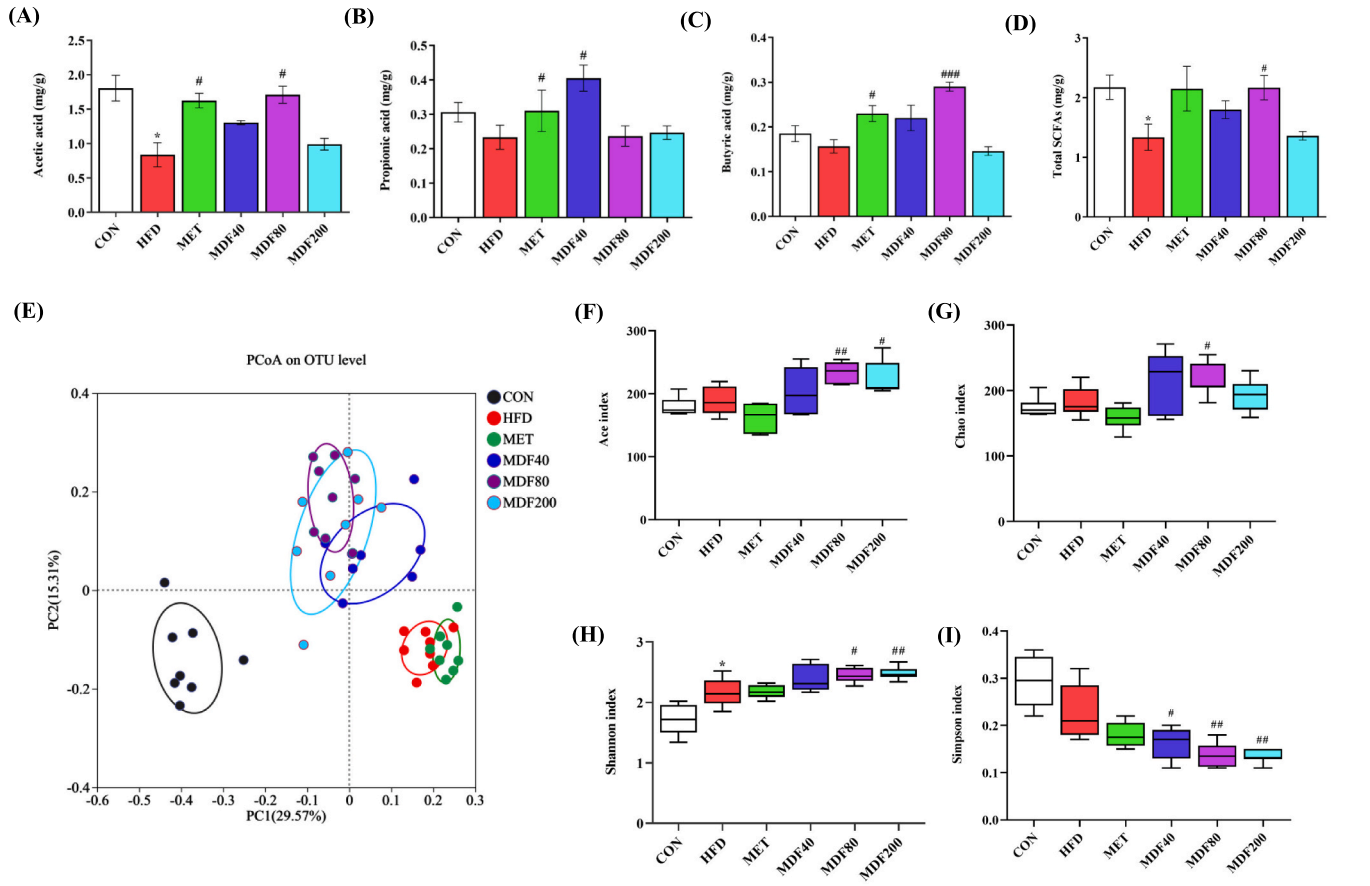

Fig. 5. Effect of MDFs on fecal short chain fatty acids (SCFAs) and microbiota diversity in mice. (A) acetic acid (B) propionic acid (C) butyric acid (D) total SCFAs. (E) Principal coordinate analysis (PCA) of intestinal microbes in mice. Alpha diversity analysis at the OTU level of microbiota in mice feces: (F) Ace index, (G) Chao index, (H) Shannon index and (I) Simpson index. Data were presented as mean ± SEM (n = 8). CON, Control group; HFD, diabetic model group; MET, positive control group, MDF40, MDF80 and MDF200, *M. oleifera* leaf dietary fiber treatment groups. $^{*}P < 0.05$ compared with CON, $^{\#}P < 0.05$, $^{\#\#}P < 0.01$ and $^{\#\#\#}P < 0.001$ compared with HFD.

all MDF groups. In addition, the relative abundance of *Bifidobacterium* was significantly increased in MDF80. Therefore, it could be speculated that dietary intake of MDFs may improve the dysregulation of intestinal flora in T2DM mice.

At the species level, compared to the control group, the relative abundance of *Ileibacterium valens* and uncultured bacterium g_*Desulfovibrio* were significantly decreased in HFD group, while largely reversed after all MDF interventions and MDF80 intervention, respectively (Fig. S4C). The relative abundance of uncultured bacterium g_*Dubosiella* was significantly increased, while further improved after MDF interventions. The relative abundance of *Lactobacillus johnsonii*, *Lactobacillus murinus* and unclassified f_*Lachnospiraceae* were significantly increased in HFD group, while fell back after all MDF interventions. Compared to the HFD group, the relative abundance of *Faecalibaculum rodentium* and uncultured bacterium g_*Coriobacteriaceae* UCG-002 were significantly improved by MDF80 and MDF200 interventions, and only by MDF80 intervention, respectively. These results indicated that diabetes-induced microbiota disturbance was reversed and converged by MDF interventions.

In order to explore the potential functional relationship between intestinal microbiota and physiological/biochemical indexes in mice, spearman correlation analysis was conducted at genus level (Fig. 6F). The GPR43/β-actin, pAMPK/AMPK, pAkt/Akt, GLP-1, insulin, PI3K/β-actin, SOD and GSH-Px were positively correlated with the beneficial bacterium *Ileibacterium*. Most of the indicators were negatively correlated with *Clostridium_sensu_stricto*_1, unclassified f_*Lachnospiraceae* and *Lactobacillus*. Among the indicators, GLP-1, PI3K/β-actin, SOD and GSH-Px were also positively correlated with the beneficial bacterium *Desulfovibrio* and *Bifidobacterium*. The HOMA-IR, TC, LDL-C, FBG, GTT, ITT, MDA and TG were positively correlated with the *Clostridium_sensu_stricto*_1, most of which also positively correlated with *Romboutsia* and unclassified f_*Lachnospiraceae*. As expected, most of these parameters were negatively correlated with *Ileibacterium*. In addition, the pErk/Erk was negatively correlated with two genera (*Romboutsia and Bifidobacterium*).

4. Discussion

MDF is mainly composed of cellulose, hemicellulose and lignin, which is similar to the dietary fibers extracted from other plant sources. The dietary fiber content of MDF was comparable to the dietary fiber from ginseng (IDF of 68.61 %) (Hua et al., 2019), bamboo shoot (TDF of 74.50 % and IDF of 73.40 %) (Li et al., 2018) and deoiled cumin (TDF of 75.58 % and IDF of 67.73, prepared by enzymatic hydrolysis) (Ma & Mu, 2016). For natural dietary fibers, the extraction process probably causes the breakdown of a few glycosidic bonds which results in the fractured amorphous region (Zheng et al., 2022). Meanwhile, a small amount of phenol and ester substances may be bound with the insoluble dietary fiber of *Moringa*. The structure of MDF was changed to the active form to facilitate its physiological effects (Zhang et al., 2024). Consequently, the extracted MDF showed a porous surface structure and better functional properties. The chemical structure of dietary fiber had a great impact on its hydration (Benitez et al., 2019; Luo et al., 2017). Thus, the WHC of MDFs was better than that of rice bran dietary fibers (2.60–3.60 g/g)

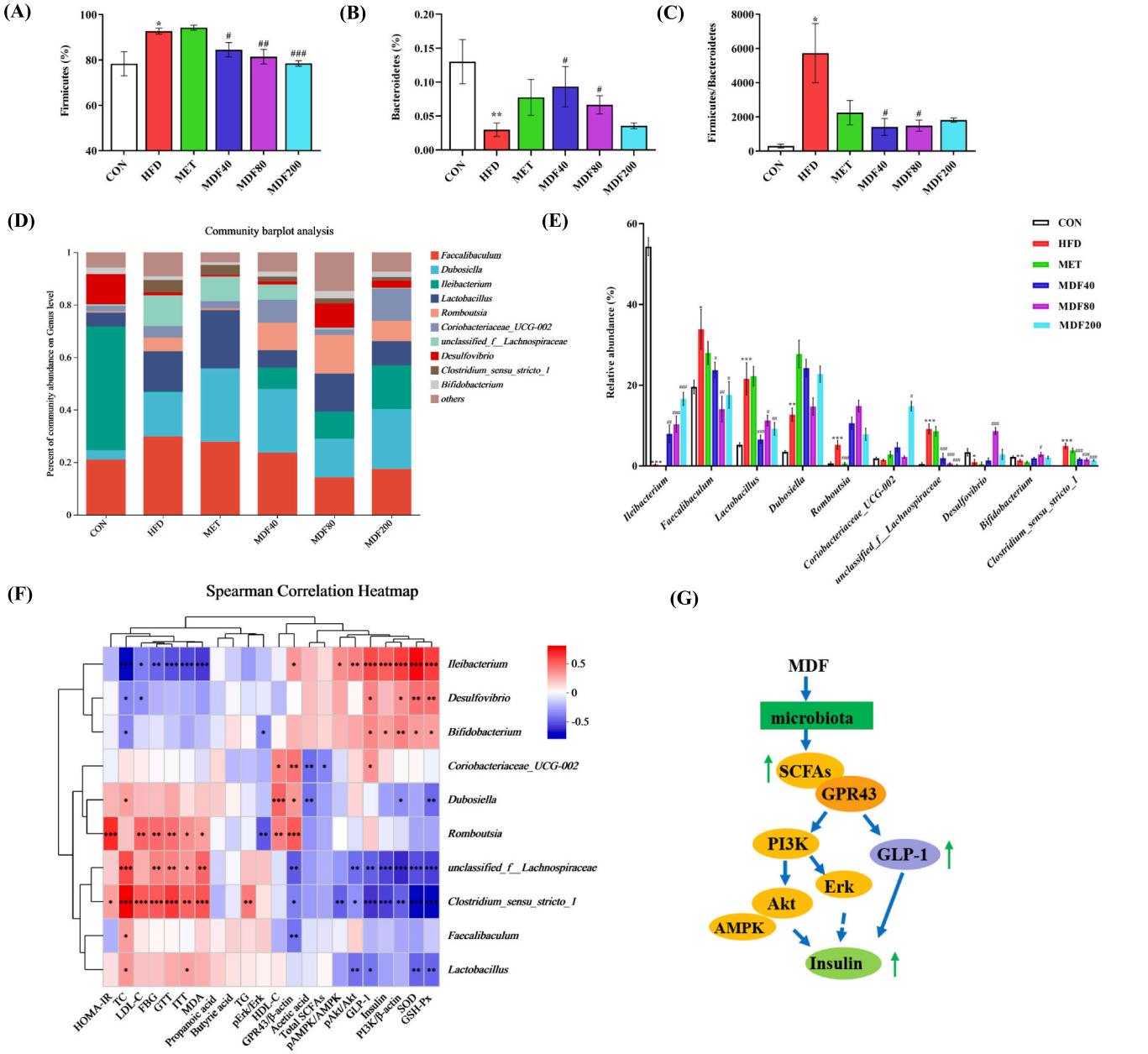

Fig. 6. Microbial abundance and its correlation with physiological indexes. The relative abundance of Firmicutes (A), Bacteroidetes (B) and the Firmicutes/Bacteroidetes ratio (C). Heat map at genus level (D) and relative abundance of top10 genus (E). Correlation between gut microbiota (genus level) and physiological parameters in T2DM mice (A). The Scheme of the the effect of MDF on physiological indexes with diabetes (B). Data were presented as mean ± SEM (n = 8). CON, control group; HFD, diabetic model group; MET, positive control group, MDF40, MDF80 and MDF200, *M. oleifera* leaf dietary fiber treatment groups. $^{*}P < 0.05$,$^{**}P < 0.01$, $^{***}P < 0.001$ compared to CON, and $^{\#}P < 0.05$, $^{\#\#}P < 0.01$, $^{\#\#\#}P < 0.001$ compared with HFD.

(Wen et al., 2017), cumin DF (3.38 g/g) (Ma & Mu, 2016), bamboo shoot DF (2.83 g/g) (Yu et al., 2023) and coffee parchment IDF (3.50 g/g) (Benitez et al., 2019). High hydration usually meant high dissolution or expansion of dietary fiber in small intestine (Benitez et al., 2019). OHC of MDF was higher than the rice bran dietary fibers (1.30–2.70 g/g) (Wen et al., 2017) and ginseng-IDF (1.78 g/g) (Hua et al., 2019), which might be beneficial to the transport of lipid in the small intestine.

Studies have confirmed that postprandial hyperglycemia is delayed by dietary fiber through glucose absorption, increased satiety or reduced total energy intake (Li & Ma, 2024; Yang et al., 2021). All tested MDFs showed inhibitory effects on α-amylase, α-glucosidase and pancreatic lipase with a size-dependent manner. The glucose adsorption capacity of MDF was similar to the trend of ginseng-IDF (Hua et al., 2019) and pea IDF (Li, Liu, et al., 2022). Similarly, the GAC of pea IDF also increased with the decreasing of particle size (Li, Liu, et al., 2022), with the strongest inhibition of glucose diffusion (2.71–36.15 %) of the smallest particle size. This was due to the increase of contact area and glucose adsorption sites between glucose and dietary fiber particles. High GAC of dietary fiber may assist to maintain glucose level in intestinal lumen and thus attenuating postprandial hyperglycemia (Li, Liu, et al., 2022). IDF was reported to reduce the concentration of glucose in intestine by absorbing glucose and delaying the diffusion of glucose, thus reducing the postprandial blood glucose level (Yang et al., 2021). Higher GDRI of dietary fiber was reported to benefit for the control of blood glucose through delaying the adsorption of glucose in the gastrointestinal tract (Benitez et al., 2019; Nsor-Atindana et al., 2012). This may be related to the unique composition of cellulose and hemicellulose in MDF (Table 1 and Fig. S2).

Previous studies reported that the inhibition effect of dietary fibers on digestive enzymes was mainly determined by their internal structure and surface properties (Wu et al., 2020; Yang et al., 2021). More functional group exposure of MDF200 during grinding facilitates embedding the active site of α-glucosidase, α-amylase and pancreatic lipase. Similarly, the smaller the particle size of IDF of corn bran, the better the inhibition activities of α-glucosidase and α-amylase (Jiang et al., 2022). Therefore, it could be speculated that the inhibition effects of MDF was attributed not only to their loose and spatial network structure (Fig. S21) for substrates such as glucose molecule, starch and lipid or hydrolase capsulation, but also their high water and oil holding capacities for the increasing solution viscosity, which led to delaying of starch diffusion or affinity reduction of α-amylase to the starch substrate. Dietary fiber from coffee parchment (rich in hemicellulosic and cellulosic polysaccharides) adsorbed amylase and retard the digestion of starch (Benitez et al., 2019). The IDF from *Sea buckthorn* seed obtained by ball milling combined with cellulase treatment showed a good inhibitory effect on starch digestion (Zhu et al., 2022). The inhibition effect of MDFs on pancreatic lipase is increased with smaller particle size, which may be caused by the fact that the smaller particle size leads to more exposure of hydrophobic groups, which increases the affinity and contact area with oil. The inhibition effect of MDFs on pancreatic lipase was similar to that of soluble dietary fibers from *Akebia trifoliata* (Thunb.) Koidz. Seeds (22.6–33.7 %) using ultrasonication/shear emulsifying/microwave-assisted enzymatic extraction (Jiang et al., 2020). The inhibitory effect of IDF from citrus peel on pancreatic lipase also showed increasing trend with the decrease of particle size (Yu et al., 2023).

Persistent hyperglycemia and impaired glucose tolerance are important diagnostic criteria for T2DM (He et al., 2022). Results showed the insulin resistance of T2DM mice was improved by MDF interventions, which was verified by the reduction of FBG, insulin, HOMA-IR, and the AUC of GTT and ITT. In addition to elevated blood glucose, dyslipidemia, namely hypertriglyceridemia and hypercholesterolemia, is accompanied with T2DM. Previous studies have shown that insulin resistance is the main cause of dyslipidemia (Tu et al., 2019). Therefore, alleviating insulin resistance in patients with T2DM may delay the progression of diabetes symptoms. In this study, the dyslipidemia was relieved to some extent after MDF interventions. What's more, clinical studies showed that T2DM was associated with different degrees of organ damage, such as liver and pancreas (Jia et al., 2019), which was caused by long-term excessive oxidative stress. Combined with the H&E stain observations, MDFs intake reduced oxidative stress and organ damage in T2DM mice. The activities of antioxidant enzymes (SOD and GSH-P_X) of T2DM mice were increased, meanwhile the MDA content was decreased (Fig. 2F-H). The intake of dietary fibers, such as inulin, xylan and apple pectin increased the activities of antioxidant enzyme (SOD) and decreased the MDA concentration in high-fat diet fed mice (Wen et al., 2023), thus alleviating metabolic disorders. This suggests that MDFs may protect T2DM mice from hyperglycemia-induced oxidative stress by enhancing the activity of key antioxidant enzymes and reducing lipid peroxidation products (MDA), which is identified by the inhibition of the phosphorylation of Erk in liver of T2DM mice. Liver gluconeogenesis and glycogen synthesis are improved through the AMPK pathway, namely, the activation of AMPK phosphorylation may help inhibiting gluconeogenesis in diabetic mice (Liu et al., 2019). AMPK may be involved in improving insulin resistance through an insulin-independent pathway. Therefore, MDF intake may improve insulin receptor activity and insulin signaling through activation of AMPK and AKT pathways, decreasing blood glucose levels and inhibiting glycoxenogenesis in the liver.

Intestinal flora imbalance is considered to be a significant feature of T2DM. A large number of data showed that diet is the main driver of intestinal microbial populations and functions. Dietary fiber remodels the intestinal flora unequally (Wen et al., 2023; Zhao et al., 2018) and produces a large number of metabolites such as SCFAs. Result showed that MDF effectively regulated the overall structure of microbial community in T2DM mice. MDF intervention favors the growth of *Actinobacteria*, *Desulfobacterota* and *Bacteroidetes*, but not *Firmicutes* and *Patescibacteria*. Specific intestinal flora has beneficial effects such as improving insulin resistance and regulating intestinal hormones (Huang et al., 2022), which is supported by the association analysis of mouse intestinal microbes (genus level) and mouse phenotypic indicators. *Bifidobacterium* is an important probiotic genus with a wide range of physiological activities, including SCFAs production, bacteriostatic action, endotoxin reduction, vitamin synthesis, immune regulation and adsorption of toxic substances (Deng et al., 2021), which is also considered to be beneficial to human intestinal health(Ma and Li, 2024). MDF is probably fermented by *Bifidobacterium* to produce SCFAs, which enhances intestinal barrier function and regulates glucose metabolism. The proliferation of *Bifidobacterium* lowered blood cholesterol levels by breaking down bile acids and improved lipid metabolism disorder by affecting the expression of lipid metabolism related genes and reducing pro-inflammatory factors. The genera *Clostridium_sensu_stricto*_1, *Dubosiella* and *Romboutsia* are mostly associated with obesity and obesity-related disorders (Wang et al., 2021). Among them, *Clostridium_sensu_stricto*_1 was reported as a novel biomarker of obesity/obesity resistance in the small intestine (Pang et al., 2022). However, the relative abundance of *Lactobacillus* in *db/db* mice with T2DM was promoted by microcrystalline cellulose (HFD group) but suppressed by MDF intervention, indicating that insoluble dietary fibers from *Moringa* leaf didn't benefit the growth of *Lactobacillus* bacteria. Similarly, this bacterium was also significantly decreased after Tartary buckwheat bran dietary fiber intervention (He et al., 2022).

SCFAs, the fermented products of dietary fibers, is the important signaling molecules to maintaining intestinal health and regulating blood glucose metabolism (He et al., 2022) through activating colon GPR41 or GPR43 receptors and stimulating the secretion of gastrointestinal hormone GLP-1, which can directly promote insulin secretion and inhibit glucagon secretion (Bellahcene et al., 2013; Brown et al., 2003; Wang et al., 2022). These endogenous receptors, also known as free fatty acid receptors (FFAR1, FFAR2 and FFAR3), affected the ERK, PI3K-Akt and MAPK signaling pathway, and further affected fat formation and differentiation, fatty acid synthesis, absorption and transport, and cholesterol metabolism (Brown et al., 2003; den Besten et al., 2015; Tolhurst et al., 2012). Therefore, in clinical trials, increased intake of non-digestible but fermentable carbohydrates mitigated the disease phenotype of T2DM (Prasad & Bondy, 2019). It was reported that acetic acid stimulated β-islet cells to secrete insulin by directly regulating fatty acid receptor FFAR2 (GPR41) or activating parasympathetic nervous system (Tolhurst et al., 2012; Xiong et al., 2004). Propionic acid mediated gastrointestinal hormone release, inhibit cell apoptosis, directly affect glucose-stimulated insulin release, improve insulin resistance, and maintain the quality of β-islet cells. Butyric acid can stimulate intestinal glucose-generating genes, thereby regulating glucose and lipid metabolism (Huang et al., 2022). Acetic acid and butyric acid have been shown to improve glucose homeostasis by inducing intestinal production of GLP-1 that stimulate insulin secretion (Zhao et al., 2018). Carboxymethyl wheat bran dietary fiber was reported to promote the regulation of blood glucose by stimulating gastrointestinal hormone secretions (GLP-1 and PYY) and insulin secretion (Li et al., 2021). SCFAs are also reported to activate AMPK in liver and muscle tissue, promote fatty acid oxidation, and reduce fatty acid synthesis (Liu et al., 2019). Once activated, AMPK improves insulin resistance, liver gluconeogenesis and lipogenesis, and promotes fat oxidation (Liu et al., 2019).

MDF interventions increased SCFAs secretion. The specific binding of SCFAs to GPR43 receptors stimulates GLP-1 secretion and activated AMPK/PI3K-Akt signaling to facilitate insulin secretion or sensitivity and plays a beneficial role in regulating glucose homeostasis and maintaining postprandial blood glucose levels, thereby alleviating the symptoms of diabetes (Ma & Li, 2024). In this regard, the intake of MDF40 was much more effective in promoting the secretion of fecal propionic acid and serum GLP-1 as well as the phosphorylation of AMPK

in liver. By contrast, the intake of MDF80 significantly increased fecal acetic acid, butyric acid and total SCFAs and serum GLP-1. These two MDFs significantly improved the phosphorylation of AMPK and Erk. However, MDF200 didn't significantly promote the secretion of the tested SCFAs, although MDF200 was more effective in the *in vitro* studies (WHC, GAC, GDRI as well as inhibition on starch digestion and digestive enzymes). The difference in the hypoglycemic activities of the three MDFs is likely due to their different particle sizes. The larger the particle size of the dietary fiber, the more interaction of dietary fiber with intestinal mucosa and obvious physical delay effects, which is conduced to stimulate the intestinal to secrete GLP-1. MDF40 and MDF80 also alleviated the metabolic stress caused by the high-fat diet possibly due to the isolation effect of larger particles of dietary fiber on the intestinal surface. In the intestinal tract, smaller particle size of dietary fiber may move quickly along with the chyme without sufficiently mutual contact with the intestinal mucosa, which may be more conducive to promoting the growth of diversified gut microbes and the secretion of specific SCFAs in the cecum. Small particles may expose more active sites and have strong chemical reaction with microbial metabolites. Thus, there are obvious differences in the response of multiple indicators. Therefore, the hypoglycaemic effect of MDF200 is mainly through adsorption of glucose and inhibition of digestive enzyme activities. In addition, multifactor interactions, the metabolic burden and possible side effects of long-term MDF intake will be investigated positively in the future study.

5. Conclusions

The hypoglycemic activity of *Moringa* dietary fibers (MDFs) was evaluated *in vitro* and *in vivo*. The glucose adsorption and diffusion retarding abilities, the inhibition of starch digestion and digestive enzyme activities were increased with the decreased particle size of MDF *in vitro*. The increase of FBG was alleviated by MDF interventions, along with lowered HOMA-IR, alleviated dyslipidemia and large restoration of GTT and ITT in T2DM mice. MDFs intake promoted the diversity of intestinal flora and the abundance of beneficial bacteria (*Ileibacterium* and *Bifidobacterium*), while restrained the relative abundance of harmful bacteria (*Clostridium_sensu_stricto_*1 and *Romboutsia*) in feces. The abnormal activation of Erk and MAPK in liver was restored by larger MDF intake, whereas the enhancement of GLP-1 secretion and Akt phosphorylation protein was caused by smaller MDF intake. To sum up, MDFs, especially MDF80, alleviated insulin resistance and dyslipidemia of T2DM mice by modulating microbiota-SCFAs receptor (GPR43)/AMPK signaling pathways and by stimulating GLP-1 secretion resulted in activated liver PI3K/Akt signaling pathways, facilitating the alleviation oxidative stress and regulation of glycolipid metabolism (Fig. 6G).

CRediT authorship contribution statement

Xiufen Li: Writing – original draft, Formal analysis, Conceptualization. **Jinye Yong:** Writing – original draft. **Bing Zhao:** Data curation. **Yubo Zhu:** Formal analysis. **Jia Luo:** Writing – review & editing, Validation. **Jun Sheng:** Writing – review & editing, Project administration. **Yang Tian:** Writing – review & editing, Project administration.

Declaration of competing interest

The authors declare that they have no known competing financial interests or personal relationships that could have appeared to influence the work reported in this paper.

Acknowledgement

This work was supported by Yunnan Fundamental Research Projects (202401AT070241), Yunnan Innovation Team of Food and Drug Homologous Functional Food (202305AS350025) and Cassava Industrial Technology System of China (CARS-11-YNTY).

Appendix A. Supplymentary data

Appendix A. Supplementary data

Supplementary data to this article can be found online at https://doi.org/10.1016/j.foodres.2025.116196.

Data availability

Data will be made available on request.

References

Ahmad, E., Lim, S., Lamptey, R., Webb, D. R., & Davies, M. J. (2022). Type 2 diabetes. *The Lancet, 400*(10365), 1803–1820. https://doi.org/10.1016/s0140-6736(22)01655-5

Ahmed, F., Sairam, S., & Urooj, A. (2010). *In vitro* hypoglycemic effects of selected dietary fiber sources. *Journal of Food Science and Technology, 48*(3), 285–289. https://doi.org/10.1007/s13197-010-0153-7

Anwar, F., Latif, S., Ashraf, M., & Gilani, A. H. (2007). *Moringa oleifera*: A food plant with multiple medicinal uses. *Phytotherapy Research, 21*, 17–25. https://doi.org/10.1002/ptr.2023

Association of Official Analytical Chemists. (2005). *Official methods of analysis of AOAC international* (18th ed.). MD, USA: Gaithersburg.

Bellahcene, M., O'Dowd, J. F., Wargent, E. T., Zaibi, M. S., Hislop, D. C., Ngala, R. A., & Arch, J. R. S. (2013). Male mice that lack the G-protein-coupled receptor GPR41 have low energy expenditure and increased body fat content. *British Journal of Nutrition, 109*(10), 1755–1764. https://doi.org/10.1017/s0007114512003923

Benitez, V., Rebollo-Hernanz, M., Hernanz, S., Chantres, S., Aguilera, Y., & Martin-Cabrejas, M. A. (2019). Coffee parchment as a new dietary fiber ingredient: Functional and physiological characterization. *Food Research International, 122*, 105–113. https://doi.org/10.1016/j.foodres.2019.04.002

den Besten, G., Bleeker, A., Gerding, A., van Eunen, K., Havinga, R., van Dijk, T. H., & Bakker, B. M. (2015). Short-chain fatty acids protect against high-fat diet-induced obesity via a PPARγ-dependent switch from lipogenesis to fat oxidation. *Diabetes, 64*(7), 2398–2408. https://doi.org/10.2337/db14-1213

Brown, A. J., Goldsworthy, S. M., Barnes, A. A., Eilert, M. M., Tcheang, L., Daniels, D., & Dowell, S. J. (2003). The orphan G protein-coupled receptors GPR41 and GPR43 are activated by propionate and other short chain carboxylic acids. *Journal of Biological Chemistry, 278*(1), 11312–11319. https://doi.org/10.1074/jbc.m211609200

Chen, C., Zhang, B., Huang, Q., Fu, X., & Liu, R. H. (2017). Microwave-assisted extraction of polysaccharides from *Moringa oleifera* Lam. Leaves: Characterization and hypoglycemic activity. *Industrial Crops and Products, 100*, 1–11. https://doi.org/10.1016/j.indcrop.2017.01.042

Deng, Z., Wu, N., Wang, J., & Zhang, Q. (2021). Dietary fibers extracted from *Saccharina japonica* can improve metabolic syndrome and ameliorate gut microbiota dysbiosis induced by high fat diet. *Journal of Functional Foods, 85*, Article 104642. https://doi.org/10.1016/j.jff.2021.104642

Emaga, T. H., Robert, C., Ronkart, S. N., Wathelet, B., & Paquot, M. (2008). Dietary fibre components and pectin chemical features of peels during ripening in banana and plantain varieties. *Bioresource Technology, 99*(10), 4346–4354. https://doi.org/10.1016/j.biortech.2007.08.030

Grosshagauer, S., Pirkwieser, P., Kraemer, K., & Somoza, V. (2021). The future of Moringa foods: A food chemistry perspective. *Frontiers in Nutrition, 8*, 751076. https://doi.org/10.3389/fnut.2021.751076

Gu, F., Tao, L., Chen, R., Zhang, J., Wu, X., Yang, M., & Tian, Y. (2022). Ultrasonic-cellulase synergistic extraction of crude polysaccharides from *Moringa oleifera* leaves and alleviation of insulin resistance in HepG2 cells. *International Journal of Molecular Sciences, 23*(20), 12405. https://doi.org/10.3390/ijms232012405

He, X., Li, W., Chen, Y., Lei, L., Li, F., Zhao, J., & Ming, J. (2022). Dietary fiber of Tartary buckwheat bran modified by steam explosion alleviates hyperglycemia and modulates gut microbiota in *db/db* mice. *Food Research International, 157*, Article 111386. https://doi.org/10.1016/j.foodres.2022.111386

Hsu, Y.-L., Chen, C.-C., Lin, Y.-T., Wu, W.-K., Chang, L.-C., Lai, C.-H., & Kou, C.-H. (2019). Evaluation and optimization of sample handling methods for quantification of short-chain fatty acids in human fecal samples by GC-MS. *Journal of Proteome Research, 18*(5), 1948–1957. https://doi.org/10.1021/acs.jproteome.8b00536

Hua, M., Lu, J., Qu, D., Liu, C., Zhang, L., Li, S., & Sun, Y. (2019). Structure, physicochemical properties and adsorption function of insoluble dietary fiber from ginseng residue: A potential functional ingredient. *Food Chemistry, 286*, 522–529. https://doi.org/10.1016/j.foodchem.2019.01.114

Huang, H., Chen, J., Chen, Y., Xie, J., Xue, P., Ao, T., & Yu, Q. (2022). Metabonomics combined with 16S rRNA sequencing to elucidate the hypoglycemic effect of dietary fiber from tea residues. *Food Research International, 155*, Article 111122. https://doi.org/10.1016/j.foodres.2022.111122

Isken, F., Klaus, S., Osterhof, M., Pfeifer, A. F., & Weickert, M. O. (2010). Efects of long-term soluble *vs.* insoluble dietary fiber intake on high-fat diet-induced obesity in C57BL/6J mice. *The Journal of Nutritional Biochemistry, 21*, 278–284. https://doi.org/10.1016/j.jnutbio.2008.12.012

Jia, W., Weng, J., Zhu, D., Ji, L., Lu, J., Zhou, Z., & Zhao, Z. (2019). Standards of medical care for type 2 diabetes in China 2019. *Diabetes/Metabolism Research and Reviews, 35*(6), 3158–3166. https://doi.org/10.1002/dmrr.3158

Jiang, C., Wang, R., Liu, X., Wang, J., Zheng, X., & Zuo, F. (2022). Effect of particle size on physicochemical properties and in vitro hypoglycemic ability of insoluble dietary fiber from corn bran. *Frontiers in Nutrition, 9*, Article 951821. https://doi.org/10.3389/fnut.2022.951821

Jiang, Y., Yin, H., Zheng, Y., Wang, D., Liu, Z., Deng, Y., & Zhao, Y. (2020). Structure, physicochemical and bioactive properties of dietary fibers from *Akebia trifoliata* (Thunb.) Koidz. Seeds using ultrasonication/shear emulsifying/microwave-assisted enzymatic extraction. *Food Research International, 136*, Article 109348. https://doi.org/10.1016/j.foodres.2020.109348

Jin, R., Guo, Y., Xu, B., Wang, H., & Yuan, C. (2019). Physicochemical properties of polysaccharides separated from *Camellia oleifera* Abel seed cake and its hypoglycemic activity on streptozotocin-induced diabetic mice. *International Journal of Biological Macromolecules, 125*, 1075–1083. https://doi.org/10.1016/j.ijbiomac.2018.12.059

Li, L., Ma, L., Wen, Y., Xie, J., Yan, L., Ji, A., & Sheng, J. (2022). Crude polysaccharide extracted from *Moringa oleifera* leaves prevents obesity in association with modulating gut microbiota in high-fat diet-fed mice. *Frontiers in Nutrition, 9*, Article 861588. https://doi.org/10.3389/fnut.2022.861588

Li, M., & Ma, S. (2024). A review of healthy role of dietary fiber in modulating chronic diseases. *Food Research International, 27*, Article 114682. https://doi.org/10.1016/j.foodres.2024.114682

Li, X., Fu, B., Guo, J., Ji, K., Xu, Y., Dabab, M. M., & Zhang, P. (2018). Bamboo shoot fiber improves insulin sensitivity in high-fat diet-fed mice. *Journal of Functional Foods, 49*, 510–517. https://doi.org/10.1016/j.jff.2018.09.016

Li, X., Guo, J., Ji, K., & Zhang, P. (2016). Bamboo shoot fiber prevents obesity in mice by modulating the gut microbiota. *Scientific Reports, 6*, 32953. https://doi.org/10.1038/srep32953

Li, X., Zhang, X., Zhang, R., Ni, Z., Elam, E., Thakur, K., & Wei, Z. (2021). Gut modulation based anti-diabetic effects of carboxymethylated wheat bran dietary fiber in high-fat diet/streptozotocin-induced diabetic mice and their potential mechanisms. *Food and Chemical Toxicology, 152*, Article 112235. https://doi.org/10.1016/j.fct.2021.112235

Li, Y., Liu, J., Zhang, Y., Wang, Q., & Wang, J. (2022). Qualitative and quantitative correlation of microstructural properties and *in vitro* glucose adsorption and diffusion behaviors of pea insoluble dietary fiber induced by ultrafine grinding. *Foods, 11*(18), 2814. https://doi.org/10.3390/foods11182814

Li, Y., Teng, D., Shi, X., Qin, G., Qin, Y., Quan, H., & Shan, Z. (2020). Prevalence of diabetes recorded in mainland China using 2018 diagnostic criteria from the American Diabetes Association: National cross sectional study. *The BMJ, 369*, Article m997. https://doi.org/10.1136/bmj.m997

Liu, H., Qi, X., Yu, K., Lu, A., Lin, K., Zhu, J., & Sun, Z. (2019). AMPK activation is involved in hypoglycemic and hypolipidemic activities of mogroside-rich extract from *Siraitia grosvenorii* (Swingle) fruits on high-fat diet/streptozotocin-induced diabetic mice. *Food & Function, 10*(1), 151–162. https://doi.org/10.1039/c8fo01486h

Luo, X., Wang, Q., Zheng, B., Lin, L., Chen, B., Zheng, Y., & Xiao, J. (2017). Hydration properties and binding capacities of dietary fibers from bamboo shoot shell and its hypolipidemic effects in mice. *Food and Chemical Toxicology, 109*, 1003–1009. https://doi.org/10.1016/j.fct.2017.02.029

Lyu, B., Wang, Y., Zhang, X., Chen, Y., Fu, H., Liu, T., & Jiang, L. (2021). Changes of high-purity insoluble fiber from soybean dregs (Okara) after being fermented by colonic flora and its adsorption capacity. *Foods, 10*(10), 2485. https://doi.org/10.3390/foods10102485

Ma, M.-M., & Mu, T.-H. (2016). Effects of extraction methods and particle size distribution on the structural, physicochemical, and functional properties of dietary fiber from deoiled cumin. *Food Chemistry, 194*, 237–246. https://doi.org/10.1016/j.foodchem.2015.07.095

Ma, S., & Li, M. (2024). A review of healthy role of dietary fiber in modulating chronic diseases. *Food Research International, 191*, Article 114682. https://doi.org/10.1016/j.foodres.2024.114682

Mallillin, A. C., Trinidad, T. P., Sagum, R. S., de Leon, M. P., Borlagdan, M. P., Baquiran, A. F. P., & Aviles, T. F. (2014). Mineral availability and dietary fiber characteristics of *Moringa oleifera*. *Food and Public Health, 4*(5), 242–246. https://doi.org/10.5923/j.fph.20140405.05

Nsor-Atindana, J., Zhong, F., & Mothibe, K. J. (2012). *In vitro* hypoglycemic and cholesterol lowering effects of dietary fiber prepared from cocoa (*Theobroma cacao* L.) shells. *Food & Function, 3*(10), 1044. https://doi.org/10.1039/c2fo30091e

Pang, Y., Zheng, Y., Yang, N., Zan, M., Zhang, L., & Ding, W. (2022). Potential novel biomarkers in small intestine for obesity/obesity resistance revealed by multi-omics analysis. *Lipids in Health and Disease, 21*, 98. https://doi.org/10.1186/s12944-022-01711-0

Prasad, K. N., & Bondy, S. C. (2019). Dietary fibers and their fermented short-chain fatty acids in prevention of human diseases. *Mechanisms of Ageing and Development, 17*, Article 100170. https://doi.org/10.1016/j.mad.2018.10.003

Rumpf, J., Burger, R., & Schulze, M. (2023). Statistical evaluation of DPPH, ABTS, FRAP, and Folin-ciocalteu assays to assess the antioxidant capacity of lignins. *International Journal of Biological Macromolecules, 233*, Article 123470. https://doi.org/10.1016/j.ijbiomac.2023.123470

Somoza, V., Pirkwieser, P., Grosshagauer, S., & Kraemer, K. (2021). The future of Moringa foods: A food chemistry perspective. *Frontiers in Nutrition, 8*, Article 751076. https://doi.org/10.3389/fnut.2021.751076

Thomas, R. L., Halim, S., Gurudas, S., Sivaprasad, S., & Owens, D. R. (2019). IDF diabetes atlas: A review of studies utilising retinal photography on the global prevalence of diabetes related retinopathy between 2015 and 2018. *Diabetes Research and Clinical Practice, 157*, Article 107840. https://doi.org/10.1016/j.diabres.2019.107840

Tolhurst, G., Heffron, H., Lam, Y. S., Parker, H. E., Habib, A. M., Diakogiannaki, E., & Gribble, F. M. (2012). Short-chain fatty acids stimulate glucagon-like peptide-1 secretion via the G-protein-coupled receptor FFAR2. *Diabetes, 61*(2), 364–371. https://doi.org/10.2337/db11-1019

Tu, J., Liu, G., Cao, X., Zhu, S., Li, Q., Ji, G., & Xiao, G. (2019). Hypoglycemic effects of wheat bran alkyresorcinols in high-fat/high-sucrose diet and low-dose streptozotocin-induced type 2 diabetic male mice and protection of pancreatic β cells. *Food & Function, 10*(6), 3282–3290. https://doi.org/10.1039/c8fo02396d

Vargas-Sánchez, K., Garay-Jaramillo, E., & González-Reyes, R. E. (2019). Effects of *Moringa oleifera* on glycaemia and insulin levels: A review of animal and human studies. *Nutrients, 11*(12), 2907. https://doi.org/10.3390/nu11122907

Wang, M., Yang, F., Yan, X., Chao, X., Zhang, W., Yuan, C., & Zeng, Q. (2022). Anti-diabetic effect of banana peel dietary fibers on type 2 diabetic mellitus mice induced by streptozotocin and high-sugar and high-fat diet. *Journal of Food Biochemistry, 46*(10), 14275. https://doi.org/10.1111/jfbc.14275

Wang, Y., Ablimit, N., Zhang, Y., Li, J., Wang, X., Liu, J., & Jiang, W. (2021). Novel β-mannanase/GLP-1 fusion peptide high effectively ameliorates obesity in a mouse model by modifying balance of gut microbiota. *International Journal of Biological Macromolecules, 191*, 753–763. https://doi.org/10.1016/j.ijbiomac.2021.09.150

Wen, J.-J., Li, M.-Z., Hu, J.-L., Wang, J., Wang, Z.-Q., Chen, C.-H., & Hie, S.-P. (2023). Different dietary fibers unequally remodel gut microbiota and charge up anti-obesity effects. *Food Hydrocolloids, 140*, Article 108617. https://doi.org/10.1016/j.foodhyd.2023.108617

Wen, Y., Niu, M., Zhang, B., Zhao, S., & Xiong, S. (2017). Structural characteristics and functional properties of rice bran dietary fiber modified by enzymatic and enzyme-micronization treatments. *LWT - Food Science and Technology, 75*, 344–351. https://doi.org/10.1016/j.lwt.2016.09.012

Wu, W., Hu, J., Gao, H., Chen, H., Fang, X., Mu, H., & Liu, R. (2020). The potential cholesterol-lowering and prebiotic effects of bamboo shoot dietary fibers and their structural characteristics. *Food Chemistry, 332*, Article 127372. https://doi.org/10.1016/j.foodchem.2020.127372

Xiang, Z., Xie, H., Tong, Q., Pan, J., Wan, L., Fang, J., & Chen, J. (2021). Revealing hypoglycemic and hypolipidemic mechanism of Xiaokeyinshui extract combination on streptozotocin-induced diabetic mice in high sucrose/high fat diet by metabolomics and lipidomics. *Biomedicine & Pharmacotherapy, 135*, Article 111219. https://doi.org/10.1016/j.biopha.2021.111219

Xiong, Y., Miyamoto, N., Shibata, K., Valasek, M. A., Motoike, T., Kedzierski, R. M., & Yanagisawa, M. (2004). Short-chain fatty acids stimulate leptin production in adipocytes through the G protein-coupled receptor GPR41. *Proceedings of the National Academy of Sciences of the United States of America, 101*(4), 1045–1050. https://doi.org/10.1073/pnas.2637002100

Xu, J., Liu, T., Li, Y., Yuan, C., Ma, H., Seeram, N. P., & Li, L. (2018). Hypoglycemic and hypolipidemic effects of triterpenoid-enriched Jamun (*Eugenia jambolana* Lam.) fruit extract in streptozotocin-induced type 1 diabetic mice. *Food & Function, 9*(6), 3330–3337. https://doi.org/10.1039/c8fo00095f

Xue, Z., Gao, X., Jia, Y., Wang, Y., Lu, Y., Zhang, M., … Chen, H. (2020). Structure characterization of high molecular weight soluble dietary fiber from mushroom *Lentinula edodes* (Berk.) pegler and its interaction mechanism with pancreatic lipase and bile salts. *International Journal of Biological Macromolecules, 153*, 1281–1290. https://doi.org/10.1016/j.ijbiomac.2019.10.263

Yang, M., Tao, L., Kang, X. R., Wang, Z. L., Su, L. Y., Li, L. F., & Tian, Y. (2023). *Moringa oleifera* Lam. Leaves as new raw food material: A review of its nutritional composition, functional properties, and comprehensive application. *Trends in Food Science & Technology, 138*, 399–416. https://doi.org/10.1016/j.tifs.2023.05.013

Yang, X., Dai, J., Zhong, Y., Wei, X., Wu, M., Zhang, Y., & Xiao, H. (2021). Characterization of insoluble dietary fiber from three food sources and their potential hypoglycemic and hypolipidemic effects. *Food & Function, 12*(14), 6576–6587. https://doi.org/10.1039/d1fo00521a

Yang, X., Lin, L., & Zhao, M. (2023). Preparation, chemical composition, glycolipid-lowering activity and functional property of high-purity polysaccharide from *Moringa oleifera Lam*. Leaf: A novel plant-based functional hydrophilic colloid. *Food Hydrocolloids, 142*, Article 108857. https://doi.org/10.1016/j.foodhyd.2023.108857

Yu, B., Tang, Q., Fu, C., Regenstein, J., Huang, J., & Wang, L. (2023). Effects of different particle-sized insoluble dietary fibre from citrus peel on adsorption and activity inhibition of pancreatic lipase. *Food Chemistry, 398*, Article 133834. https://doi.org/10.1016/j.foodchem.2022.133834

Zhang, G., Wang, D., Ding, Y., Zhang, J., Ding, Y., & Lyu, F. (2024). Effect and mechanism of insoluble dietary fiber on postprandial blood sugar regulation. *Trends in Food Science & Technology, 146*, Article 104354. https://doi.org/10.1016/j.tifs.2024.104354

Zhao, L., Zhang, F., Ding, X., Wu, G., Lam, Y. Y., Wang, X., & Zhang, C. (2018). Gut bacteria selectively promoted by dietary fibers alleviate type 2 diabetes. *Science, 359* (6380), 1151–1156. https://doi.org/10.1126/science.aao5774

Zheng, Y., Xu, B., Shi, P., Tian, H., Li, Y., Wang, X., & Liang, P. (2022). The influences of acetylation, hydroxypropylation, enzymatic hydrolysis and crosslinking on improved adsorption capacities and *in vitro* hypoglycemic properties of millet bran dietary fibre. *Food Chemistry, 368*, Article 130883. https://doi.org/10.1016/j.foodchem.2021.130883

Zhu, Y., Ji, X., Yuen, M., Yuen, T., Yuen, H., Wang, M., & Peng, Q. (2022). Effects of ball milling combined with cellulase treatment on physicochemical properties and *in vitro* hypoglycemic ability of sea buckthorn seed meal insoluble dietary fiber. *Frontiers in Nutrition, 8*, Article 820672. https://doi.org/10.3389/fnut.2021.820672